Manuscript ade5725-R2

Myeloid cell-derived proteases produce a pro-inflammatory form of IL-37 that signals via IL-36 receptor engagement

Graeme P. Sullivan,[1,7#] Pavel Davidovich,[1#] Natalia Muñoz-Wolf,[2] Ross W. Ward,[2] Yasmina E. Hernandez Santana,[3,4] Danielle M. Clancy,[1,6] Aoife Gorman,[2] Zaneta Najda,[1] Boris Turk,[5] Patrick T. Walsh,[3,4] Ed C. Lavelle[2] and Seamus J. Martin[1,*]

[1]Molecular Cell Biology Laboratory, Dept. of Genetics, The Smurfit Institute, Trinity College, Dublin 2, Ireland.
[2]Adjuvant Research Group, School of Biochemistry and Immunology, Trinity Biomedical Sciences Institute, Trinity College, Dublin 2, Ireland.
[3]National Children's Research Centre, CHI-Crumlin, Dublin, Ireland
[4]Department of Clinical Medicine, School of Medicine, Trinity College, Dublin 2, Ireland
[5]Department of Biochemistry, Molecular and Structural Biology, Jožef Stefan Institute, Ljubljana, Slovenia.
[6]Present address: VIB-UGent Center for Inflammation Research, Department of Biochemistry and Microbiology, Ghent University, Ghent, Belgium.
[7]Present address: Dept. of Physiology and Medical Physics, Royal College of Surgeons in Ireland, Dublin 2, Ireland.
[#]These authors share first authorship

*Correspondence to: Seamus J. Martin, Ph.D.
Email: martinsj@tcd.ie

Abstract: Interleukin (IL)-1 family cytokines are key barrier cytokines that are typically expressed as inactive, or partially active, precursors that require proteolysis within their N-termini for activation. IL-37 is an enigmatic member of the IL-1 family that has been proposed to be activated by caspase-1 and to exert anti-inflammatory activity through engagement of the IL-18R and SIGIRR. However, here we show that the longest IL-37 isoform, IL-37b, exhibits robust pro-inflammatory activity upon N-terminal proteolysis by neutrophil elastase or cathepsin S. In sharp contrast, caspase-1 failed to process or activate IL-37 at concentrations that robustly activated its canonical substrate, IL-1β. IL-37 and IL-36 exhibit high structural homology and, consistent with this, a K53-truncated form of IL-37, mimicking the cathepsin S-processed form of this cytokine, was found to exert its pro-inflammatory effects via IL-36 receptor engagement and produced an inflammatory signature practically identical to IL-36. Administration of K53-truncated IL-37b intraperitoneally into wild type mice also elicited an inflammatory response that

was attenuated in *IL-36R*$^{-/-}$ animals. These data demonstrate that, in common with other IL-1 family members, mature IL-37 can also elicit pro-inflammatory effects upon processing by specific proteases.

One Sentence Summary: IL-37 exhibits pro-inflammatory activity via IL-36 receptor activation.

INTRODUCTION

Members of the extended IL-1 family are key barrier cytokines that act at the apex of pro-inflammatory signaling cascades in response to infection or immune barrier disruption (*1, 2*). IL-37 (IL-1F7) is expressed in humans, non-human primates and other mammals, but not rodents, and has been proposed to be anti-inflammatory, which is at odds with the pro-inflammatory effects of all other cytokines within the extended IL-1 family (*3-6*). Previous studies have proposed that IL-37 exerts its anti-inflammatory functions either via engagement of the IL-18 receptor or SIGIRR/IL-1R8, and also potentially through translocation to the nucleus where it has been suggested that IL-37 may directly suppress transcription of LPS-induced genes (*7-9*).

Because IL-1 family cytokines all contain N-terminal pro-domains that either partly or completely restrain the ability of these cytokines to activate their cognate receptors, proteases play a key role in regulating the activity of IL-1 family members (*2, 10*). For example, IL-1β, IL-18, IL-36α, IL-36β and IL-36γ are all expressed as completely inactive precursors that can be activated through N-terminal processing by specific proteases, including caspase-1, elastase, cathepsin G or cathepsin S (*10-14*). Initial studies on the longest IL-37 isoform (IL-37b) proposed that this cytokine is processed and activated by caspase-1 at Asp20 (*15*). However, it is debatable whether IL-37 is a *bona fide* substrate for caspase-1 at physiologically relevant concentrations of this protease, as caspase-1 was found to process IL-37 very inefficiently under conditions where complete processing of IL-18 was observed (*15*). Many subsequent studies on IL-37b have used artificial truncations after Asp20 that represent the putative caspase-1-processed form of this cytokine, or other truncations (predominantly after Phe45) that represent proteolysis by unidentified proteases (*9, 16-17*). Thus, the identity of the protease(s) that process IL-37 under physiological conditions and the specific residues that encompass the fully mature form of this cytokine remain uncertain.

Although caspase-1 is well established to process and activate IL-1β and IL-18, the neutrophil granule proteases – elastase, cathepsin G and proteinase-3 – have been shown to activate multiple IL-1 family cytokines, including IL-1α, IL-33, IL-36α, IL-36β and IL-36γ (*2, 10, 13, 18-20*). Neutrophils typically liberate their granule proteases in response to necrotic cells or

large aggregates of non-phagocytosable material, and are typically the first and the most numerous immunocytes to arrive at inflammatory sites (*21*). Consequently, neutrophil-derived proteases are abundant at sites of tissue injury where IL-1 family cytokines are released into the extracellular space due to necrosis. Cathepsin S, a lysosomal cysteine protease that is elevated and often secreted at inflammatory sites, particularly in the skin, has also been implicated in the processing and activation of IL-36 family cytokines (*14*). Thus, in addition to caspase-1, a paradigm has emerged whereby proteases that are released from activated myeloid cells, particularly neutrophils, serve as key activators of IL-1 family cytokines in multiple settings (*2, 10, 13, 14, 18, 20*).

Here, we explored whether proteases liberated by activated neutrophils or macrophages could process the longest IL-37 isoform, IL-37b, at physiologically relevant concentrations of these enzymes. Unexpectedly, we demonstrate that elastase- or cathepsin S-mediated processing of IL-37 produced forms of this cytokine that exhibited robust pro-inflammatory activity *in vitro* as well as *in vivo*. Furthermore, we also found that elastase- or cathepsin S-processed IL-37 promoted inflammation in an IL-36 receptor-dependent manner *in vitro* and *in vivo*. These data shed light upon the post-translational processing and activation of IL-37 and suggest that this cytokine may possess both pro- and anti-inflammatory functions dependent on the truncated forms of IL-37 produced by specific proteases.

RESULTS

Neutrophil-derived proteases process IL-37 to a pro-inflammatory form

To explore whether inflammatory proteases are capable of processing and activating IL-37, similar to their ability to process other IL-1 family cytokines, we initially assessed the activity of full-length recombinant pro-IL-37b on human HaCaT keratinocytes. Full-length IL-37 was incubated for 2 h in the presence or absence of supernatants from resting or PMA-activated human neutrophils that contain low nanomolar concentrations of elastase, cathepsin G and proteinase-3, as we have previously shown (*13, 22, 23*). IL-37 reaction products were then added to HaCaT cells overnight. As expected, full-length pro-IL-37 failed to exhibit pro-inflammatory activity, as assessed by measuring cytokine secretion from HaCaT cells, while these cells readily responded to active IL-36β (**Fig. 1A and fig. S1A and S1B**). However, IL-37 that was pre-incubated with supernatants from PMA-activated neutrophils unexpectedly exhibited robust pro-inflammatory activity, eliciting the secretion of IL-6, IL-8 and G-CSF from HaCaT cells (**Fig. 1B and fig. S1C and S1D**). Supernatants from activated neutrophils did not exhibit significant pro-inflammatory activity in the absence of IL-37 (**Fig. 1B and fig. S1C and S1D**).

Elastase-mediated processing produces active and inactive forms of IL-37

To explore the specific neutrophil protease(s) capable of processing and activating IL-37, we incubated the latter with nanomolar concentrations of purified human elastase or cathepsin G, which revealed that elastase processed and activated IL-37 (**Fig. 1, C and D and fig. S1E-G**), while Cat G processed but failed to activate the latter cytokine (**Fig. 1, E and F and fig. S1E**). Importantly, in the absence of IL-37, elastase did not elicit cytokine production from HaCaT cells over a wide concentration range (**fig. S1G and S1H**). Elastase-processed IL-37 also exhibited robust pro-inflammatory activity on primary human keratinocytes (**Fig. 1G**). Interestingly, elastase-mediated processing of IL-37 typically produced a bell shaped pattern of activation, where increasing concentrations of protease produced less active IL-37 beyond a certain concentration threshold (>5-10 nM), which is indicative of inactivating proteolysis occurring at higher protease concentrations (**Fig. 1, C and G and fig. S1F and S1G**). Elastase-treated IL-37 was processed to fragments of approximately 18, 17 and 11 kDa (**Fig. 1H**). To map the major elastase cleavage sites within IL-37, we sequenced the N-terminus of the elastase-cleaved cytokine, which indicated that elastase processed IL-37 at two major sites: Val46 and Val113 (**Fig. 1I**), as well as two additional minor cleavage sites (Thr42 and Thr48).

To explore the role of the various elastase cleavage sites in generating the pro-inflammatory form of IL-37, we generated point mutants of IL-37 where Thr42, Val46 and Val113 were alternatively mutated to Gly. The V46G IL-37 mutant resisted activation by elastase to a much greater extent than the T42G mutant (**Fig. 1J and fig. S1I**), suggesting that elastase activated IL-37 predominantly through processing after Val46. Furthermore, generation of a double T42G/V46G point mutant suppressed elastase-mediated IL-37 activation to an almost identical degree to the V46G mutant (**Fig. 1J and fig. S1I**). In sharp contrast to the effects seen upon mutation of Val46, mutation of Val113 did not suppress activation of IL-37 by elastase to any extent (**Fig. 1J fig. S1I**). However, the V113 point mutant exhibited considerably more robust IL-37 activity at higher concentrations of elastase, compared with wild type IL-37 (**Fig. 1K**). This suggests that processing at Val113 inactivates IL-37, which is consistent with this cleavage site being located within the IL-37 cytokine domain (**Fig. 1I**) and is also consistent with our observations that higher concentrations of elastase were less effective in producing active IL-37, as noted earlier (**Fig. 1, C and G**).

To further explore the functional importance of the multiple elastase cleavage sites within IL-37, we also generated deletion mutants of IL-37 after Thr42, Val46, Thr48 and Val113 through insertion of a caspase-3 cleavage motif (DEVD) after these residues, thereby enabling the generation of IL-37 truncations after each of the individual elastase cleavage sites upon incubation with caspase-3 (**Fig. 1L**). Truncation of IL-37 after Thr42, Val46 or Thr48 all resulted in increased pro-inflammatory activity, with truncation after Thr42 generating relatively modest activity compared with truncation after Val46 or Thr48 (**Fig. 1L and fig. S2A and S2B**). In sharp contrast, truncation after Val113 did not generate an active form of IL-37, consistent with this being an inactivating cleavage site due to its location within the IL-37 cytokine domain (**Fig. 1, K and L and fig. S2A and S2B**). Collectively, these data suggest that elastase can activate IL-37 through processing after either: Thr42, Val46, or Thr48, with Val46 being the predominant cleavage site utilized at low nanomolar concentrations of elastase. In addition, although elastase can also cleave IL-37 after Val113, this appears to be an inactivating cleavage site that may only undergo significant proteolysis at higher concentrations of elastase (**Fig. 1K**).

Cathepsin S-mediated processing can also generate a pro-inflammatory form of IL-37

Recent studies have also implicated the elastase-like protease, cathepsin S (Cat S), in processing and activation of IL-36γ (*14*), and we also observed robust processing and activation of IL-37 upon incubation with Cat S (**Fig. 2, A and B and fig. S2C**). Comparison of the IL-37 cleavage products after incubation of the latter with elastase or Cat S suggested that these

proteases cleaved at distinct sites within IL-37, with Cat S-cleaved IL-37 running at a slightly lower molecular weight than elastase-cleaved IL-37 (**Fig. 2, B and C**). We mapped the Cat S processing sites within IL-37 by N-terminal sequencing and two major sites were found after His47 and Val52 (**Fig. 2D**). Mutation of Val52 to Gly resulted in a form of IL-37 that completely resisted activation by cathepsin S (**Fig. 2E**) and also resisted Cat S-mediated proteolysis to a significant extent (**Fig. 2F**). However, the latter mutant was still robustly activated by elastase (**Fig. 2E and fig. S2D**), demonstrating that the Val52>Gly mutant was still capable of activation at alternative processing sites. Of note, the Val52 cleavage site is widely conserved among primates and other mammals, whereas the elastase cleavage sites at Val46 or Thr48 were less well-conserved (**Fig. 2G)**.

We next generated a form of IL-37b truncated at the Cat S-processing site by removing the N-terminal 52 amino acids and inserting a caspase-3 cleavage motif (DEVD) upstream of Lys53 (**Fig. 2H**), followed by generation of K53-IL-37 through cleavage by caspase-3 (**Fig. 2I**). Of note, caspase-3 failed to process wild type IL-37 (**Fig. 2J**), but readily processed His^6-tagged DEVD-K53-IL-37 as expected (**Fig. 2I**). Whereas DEVD-K53-IL-37 was only modestly pro-inflammatory, incubation of the latter with caspase-3 to remove the DEVD motif and associated N-terminal poly-histidine purification tag, mimicking Cat S-mediated proteolysis, generated a highly pro-inflammatory form of IL-37 (**Fig. 2, K and L and fig. S2E and S2F**). Thus, elastase and Cat S are both capable of processing IL-37 within its N-terminus to produce mature forms of this cytokine that exhibit robust pro-inflammatory activity on both primary and transformed keratinocytes.

Caspase-1 fails to process IL-37 under conditions where IL-1β is robustly activated

Previous reports suggested that IL-37b is cleaved by caspase-1 after Asp20 (*5, 15*) to produce an anti-inflammatory cytokine that, among other effects, is capable of suppressing LPS-induced cytokine production from macrophages (*24*). To compare the effects of caspase-1, elastase and Cat S on the pro-inflammatory activity of IL-37, we incubated IL-37 with the latter proteases at concentrations where caspase-1 robustly processed and activated IL-1β (**Fig. 3, A-D**). However, under conditions where caspase-1 readily activated pro-IL-1β (**Fig. 3, A and B and fig. S3A-D**), IL-37 was not cleaved or activated by the latter protease, but was activated by elastase and Cat S (**Fig. 3, C and D**). Upon incubation of IL-37 at 10 to 50-fold higher concentrations of caspase-1 (500 nM), partial proteolysis of IL-37 did occur, resulting in very modest pro-inflammatory activity (**Fig. S3, A and B**). Collectively, these data suggest that IL-37 is more susceptible to proteolysis by either elastase or Cat S, compared with caspase-1. This is consistent with

previous studies, which have demonstrated that neutrophil- and macrophage-derived proteases can process and activate the majority of IL-1 family cytokines (*10, 13, 14, 18-20*), whereas processing of the latter cytokines by caspase-1 appears to be the exception rather than the rule. Furthermore, proteolysis of IL-37 by caspase-1 appears to only occur at concentrations of this protease more than 100-fold higher than those required to process IL-1β, which are unlikely to be achievable under physiological conditions.

IL-37 exhibits a pro-inflammatory signature highly similar to IL-36

To explore the pro-inflammatory signature induced by IL-37 in more detail, we incubated primary human keratinocytes with active K53-IL-37 for 2 h and conducted genome wide RNA sequencing (RNA-Seq) analysis. As a comparison, we also treated human keratinocytes with active IL-36β for the same duration. K53-IL-37 produced a robust inflammatory signature highly similar to that produced by IL-36, with IL-17C, TNF, CCL20 and IL-36γ among the most highly upregulated transcripts by both cytokines (**Fig. 3, E and F**). Furthermore, IL-37 and IL-36 also induced highly similar kinetics of IκB degradation, p65 phosphorylation and p38MAPK activation (**Fig. 3G**). These results were confirmed through measuring cytokines induced by active IL-36 and IL-37 from primary human keratinocytes (**Fig. 3H**).

IL-37 pro-inflammatory activity is IL-36 receptor-dependent

Previous reports have shown that recombinant IL-37 can interact with the α-chain of the IL-18R by *in vitro* pulldown assays, albeit with low affinity (*15, 25*). However, structural comparisons indicate that IL-37 is highly similar to IL-36γ but not IL-18 or IL-1α (**Fig. 4A**). Furthermore, our RNA-Seq analyses indicated that active K53-IL-37 promoted an inflammatory signature highly similar to that produced by IL-36 (**Fig. 3, E and F**), suggesting that IL-37 might signal via the IL-36 receptor (IL-36R). To explore this possibility, we incubated primary keratinocytes, which naturally express the IL-36R, with mature K53-IL-37 in the presence and absence of the natural IL-36R antagonist (IL-36Ra). Mature K53-IL-37-induced cytokine production in primary keratinocytes was greatly inhibited through co-incubation with IL-36Ra, suggesting that IL-37 may signal via the IL-36R (**Fig. 4B**).

We next explored the pro-inflammatory activity of IL-37 on HeLa cells, as these cells are naturally responsive to IL-1α and IL-1β but not to IL-36 family cytokines due to the absence of IL-36R expression (**Fig. S4A**) (*13*). Whereas elastase- or Cat S-processed IL-37 failed to elicit cytokine production from wild type HeLa cells, stable transfection of the latter with human IL-36R rendered these cells fully responsive to elastase-processed or Cat S-processed IL-37, but

not to full-length unprocessed IL-37 (**Fig. 4C and fig. S4, B-D**), again indicating that IL-37 signals via IL-36R engagement. Furthermore, HeLa^{IL-36R} cells were unresponsive to Cat S-treated IL-37 V52G mutant (**fig. S4B and S4C**), but were responsive to the K53 truncated form of IL-37 (**fig. S4D**), further supporting that the elastase- and Cat S-processed forms of IL-37 can signal through engagement of the IL-36R.

To explore the role of the IL-36R in propagating the pro-inflammatory effects of IL-37 further, we silenced expression of IL-36R or its co-receptor signaling chain IL-1RAcP, as well as the downstream signaling adaptor MyD88, in HaCaT cells. K53-IL-37-induced cytokine production was profoundly suppressed through knockdown of IL-36R, IL-1RAcP or MyD88, but silencing of IL-1R8/SIGIRR failed to have any effect (**Fig. 4, D and E**). In contrast, knockdown of IL-36R failed to suppress IL-1α-mediated cytokine production in the same cells, as expected (**Fig. 4F**).

Although K53-IL-37 exhibited IL-36R-dependent pro-inflammatory effects, this cytokine activated the IL-36R less efficiently than IL-36 family cytokines, as typically 20 nM of K53-IL-37 was required to achieve the same inflammatory output as 2 nM IL-36 (**Fig. 4G and fig. S4E**). This could be due to a reduced affinity of IL-37 for the IL-36R, as compared with IL-36 cytokines, or due to increased instability of IL-37. Because IL-36 and IL-37 appear to signal via the same receptor, we wondered whether IL-37 could antagonize IL-36-mediated signaling when present in excess. However, addition of several fold molar excess of IL-37 to IL-36-treated cells resulted in additive rather than antagonistic or synergistic effects of these cytokines (**Fig. 4G and fig. S4E**).

IL-36 cytokines are not required for IL-37 pro-inflammatory activity

Because IL-37 can transcriptionally upregulate IL-36γ (**Fig. 3, E and F**), it is possible that the IL-36R-dependent pro-inflammatory activity we observed was due to IL-37-induced expression and secretion of one or more IL-36 family cytokines, which then signaled via the IL-36R. However, we excluded this possibility in two ways. First, we observed that whereas addition of anti-IL-36R neutralizing antibodies to HaCaT cells prior to addition of mature active IL-37 completely suppressed the pro-inflammatory activity of the latter, addition of anti-IL-36R neutralizing antibodies 60, 90, 120 or 180 min after exposure of cells to mature IL-37 had no inhibitory effect (**Fig. 5A and fig. S5**). Similar results were also observed using IL-36γ as a positive control (**Fig. 5A and fig. S5**). The latter data argues that IL-37 signals through direct IL-36R engagement rather than through inducing the secretion of one or more IL-36 family cytokines. As a second approach, we also assessed the pro-inflammatory activity of mature K53-IL-37 in the presence

or absence of neutralizing antibodies against IL-36α, IL-36β or IL-36γ. Neutralizing antibodies directed against each of the three IL-36 subfamily cytokines failed to attenuate the pro-inflammatory activity of IL-37, but completely inhibited the pro-inflammatory activity of their target cytokines (**Fig. 5, B-D**). Furthermore, addition of anti-IL-36γ neutralizing antibodies at 0, 60 or 120 min after addition of IL-37 failed to inhibit IL-37 activity to any degree, but readily inhibited the activity of IL-36γ added concurrently (**Fig 5E**). Collectively, these data argue that mature IL-37 initiates inflammation through direct engagement of the IL-36 receptor, rather than through promoting the upregulation and secretion of one or more IL-36 family cytokines.

IL-37 can promote IL-36R-dependent inflammation in murine cells in vitro and in vivo

We next explored whether mature human K53-IL-37 was also capable of signaling via the murine IL-36 receptor. First, we assessed the activity of K53-IL-37 on murine embryonic fibroblasts as well as murine transformed 308KC keratinocytes. Whereas His^6-tagged DEVD-K53-IL-37 was inactive on murine cells as expected, processing of the latter with caspase-3 resulted in pro-inflammatory activity on murine 308KC keratinocytes as well as MEFs (**Fig. 6, A to C and fig. S6A**). Importantly, the IL-37-associated pro-inflammatory activity observed in the latter experiments was also unaffected by the LPS inhibitor polymyxin B. To explore whether active human IL-37 could also exert pro-inflammatory activity *in vivo*, we administered a dose escalation of mature K53-IL-37 into the peritoneal cavities of B6 mice and assessed peritoneal infiltrates and peritoneal cytokines after 24 h. IL-37 induced robust inflammation *in vivo*, promoting recruitment of neutrophils, eosinophils and macrophages into the peritoneal cavities of treated mice and elevated production of IL-6, KC, MIP2α, CCL20, TNFα and GMCSF detected in the peritoneal lavage from these animals (**Fig. 6, D to F and fig. S6, B and C**).

To determine whether the effects of IL-37 we observed *in vivo* were IL-36R-dependent, we repeated the previous experiments in WT versus *IL-36R*$^{-/-}$ animals. We again observed robust K53-IL-37-driven recruitment of inflammatory cells into the peritoneal cavities of WT mice, and this was substantially, but not completely, attenuated in *IL-36R*$^{-/-}$ animals (**Fig. 7, A and B)**. Furthermore, mature K53-IL-37-induced production of IL-6, KC, MIP-2, CCL20 and CCL2 *in vivo* and this was robustly attenuated in *IL-36R*$^{-/-}$ animals (**Fig. 7C**). The latter observations suggest that human mature K53-IL-37 exerts much of its pro-inflammatory effects in mice through engagement of the IL-36R. Taken together, these data demonstrate that IL-37 can be proteolytically processed and activated by physiologically-relevant concentrations of the neutrophil and macrophage proteases, elastase or cathepsin S, to produce pro-inflammatory forms of this cytokine that signal via direct IL-36R engagement.

DISCUSSION

A large body of evidence has now accumulated to suggest that members of the extended IL-1 cytokine family serve as sentinels for diverse proteases that are either liberated into the extracellular space by activated innate immune cells, such as neutrophils or mast cells, or activated intracellularly in response to infection or tissue damage (*10, 12, 14, 18-20, 26, 27*). Furthermore, accumulating evidence also suggests that IL-1 family cytokines are responsive to pathogen as well as allergen-derived proteases (*28-31*) and appear to serve as 'activity recognition receptors' for exogenous proteases or aberrant protease activity associated with infection (reviewed in *26*). Thus, the N-terminal pro-peptides of IL-1 family cytokines function as sensors for protease activity associated with pathogens, activated immune cells or homeostatic perturbations that result in inflammasome activation.

Although IL-1β and IL-18 are processed and activated by capase-1, these cytokines appear to be the exception within the extended IL-1 family, as the majority of members of this family are processed by proteases liberated from activated neutrophils, macrophages or mast cells (*10, 13, 14, 18, 19, 20, 26, 32*). Here, we have shown that IL-37 is processed and activated by elastase, a protease liberated in large quantities by activated neutrophils, as well as cathepsin S, a protease typically secreted by macrophages and keratinocytes (*33*). The pattern of proteolysis observed with elastase was somewhat complex, with three closely linked elastase cleavage sites located within the N-terminal pro-peptide of IL-37 at Thr42, Val46 and Val48, with Val46 appearing to be the most preferred elastase cleavage site. Furthermore, an additional elastase site was also mapped at Val113, but this was found to be an inactivating cleavage site, consistent with its position within the IL-37 cytokine domain. This suggests that elastase may both positively and negatively regulate the activity of IL-37 in a concentration-dependent manner. The predominant Cat S cleavage sites within IL-37 were mapped to His47 and Val52, distinct from but in very close proximity to the elastase cleavage sites. This is suggestive of a 'sensor domain' within the N-terminus of IL-37 that is highly sensitive to proteolysis by divergent proteases, similar to what has been found with IL-1α, IL-33 and IL-36 sub-family cytokines (*18, 26, 27, 29-31*). Thus, the identity of the specific proteases, as well their concentration, encountered by IL-37 at inflammatory sites may have a major bearing on the activity of this cytokine, with Cat S serving in a predominantly activating capacity. In contrast, although elastase can activate IL-37 at low nanomolar concentrations, this protease may suppress IL-37 activity at concentrations beyond this. Interestingly, several IL-1 family cytokines are also capable of becoming processed and activated by exogenous pathogen-derived proteases, which could also be true for IL-37 but was not tested in the present study (*26, 28-31*)

Previous studies on IL-37 have used a number of different forms of this cytokine, including full-length IL-37b (the longest IL-37 isoform comprising 218 amino acids) transfected into a variety of cell types or transgenically overexpressed in mice (*5, 9*), or an N-terminal truncation after Asp20, which has been proposed to be the caspase-1-cleaved form (*15*). Several previous studies have also used IL-37b truncated after Phe45 (*25*, *34-37*), a cleavage product that has been detected after overexpression of full-length IL-37 in HEK293 or CHO cells (7), as well as IL-37a truncated after Val26 (*24*), which is a form identical to the IL-37b K53 truncation (the Cat S-cleaved form of IL-37b) used for much of the present study. While it's clear that full-length IL-37 did not exhibit pro-inflammatory activity and we did not find any evidence for the generation of a pro-inflammatory form IL-37 after incubation with caspase-1 at concentrations that readily processed and activated IL-1β, it's not clear why previous studies have failed to observe the pro-inflammatory effects of mature IL-37 that we report here. One possibility is that because many of the previous studies have utilized forms of IL-37 truncated after Asp20 or Phe45, such forms of IL-37 may be only weakly pro-inflammatory, as compared with the Lys53 truncated form of this cytokine used for much of our study. Of note, we detected the most robust pro-inflammatory activity with the Cat S-cleaved form of IL-37b (aa53-218). The latter form of IL-37 was significantly more active and stable than either full-length IL-37 or other truncations between residues 42 and 48. It is also relevant to note that active forms of IL-37 were much less potent than equimolar amounts of active IL-36 cytokine preparations, possibly due to a much shorter half-life of active IL-37 or a reduced affinity for the IL-36 receptor. Interestingly, two groups have independently reported that IL-37 profoundly loses bioactivity as a consequence of end-to-end dimerization, which occurs at concentrations above ~250 nM (*34, 35*). Thus, prior studies that have explored the biological effects of IL-37 *in vitro* as well as *in vivo* may have inadvertently employed largely dimeric or other inactive forms of this cytokine through use of highly concentrated stock preparations or treatment conditions that favored the formation of dimers. An additional possibility is that prior studies have not explored the effects of mature IL-37 on cells that express high levels of IL-36 receptors, as the majority of the pro-inflammatory effects we report here were IL-36R-dependent. Finally, an additional possibility is that certain truncations of IL-37 may exert dominant-interfering effects through binding to specific IL-1 family receptors (such as IL-36R or IL-18R) but failing to productively activate these receptors, thereby acting akin to receptor antagonists.

Our observations that IL-37 can signal via IL-36 receptor engagement are compatible with observations that IL-36γ is the closest structural homologue to IL-37 within the extended IL-1 family (*34*). Furthermore, based on sequence similarity, it is likely that IL-37 arose from a

common ancestor of the IL-36 cytokines (*38, 39*) and possesses a similar ability to bind the IL-36 receptor. It is interesting to contemplate why four members of the IL-1 family—IL-36α, IL-36β, IL-36γ and IL-37—can all signal via the IL-36 receptor. One possibility is that due to the diversity of pathogens encountered at the skin barrier, a site where IL-36R-dependent activity appears to dominate, several duplications of IL-36 family cytokines have occurred to enable each member of this family to evolve distinct N-termini capable of responding to different pathogen proteases (*26, 30, 31*). Another possibility is that IL-37 has retained the ability to bind the IL-36 receptor but has also acquired other properties such as the ability to bind the IL-18R and IL-1R8/SIGIRR, thereby acquiring additional anti-inflammatory properties. In support of the latter possibility, it is relevant to note that the pro-inflammatory activity observed after administration of IL-37 *in vivo* was only partly attenuated in *IL-36R*$^{-/-}$ animals, suggesting that IL-37 may exert additional effects via alternative receptors. Further studies are clearly required to resolve the complexities of IL-37 biology.

In summary, here we have shown that elastase- or cathepsin S-processed IL-37 exhibits pro-inflammatory activity in an IL-36R-dependent manner. These data challenge the view of IL-37 as an exclusively anti-inflammatory cytokine and argue that this cytokine can exert both pro- as well as anti-inflammatory functions, possibly depending on the specific truncated forms of IL-37 produced by individual proteases.

MATERIALS AND METHODS

Study design

The objective of this study was to determine whether full-length IL-37 could be proteolytically processed and activated by proteases secreted by activated myeloid cells, including: elastase, cathepsin G and cathepsin S. We sought to determine whether IL-37 exhibited pro-inflammatory activity proteolytically processed by myeloid cell-derived proteases, similar to other members of the extended IL-1 family. Full-length recombinant IL-37 was incubated in the presence or absence of nanomolar amounts of elastase, cathepsin G, cathepsin S or caspase-1, followed by assessment of pro-inflammatory activity on HaCaT keratinocyte cells, primary human keratinocytes, HeLa wild type cells and HeLa cells stably-expressing the IL-36 receptor. We explored the receptor(s) utilised by IL-37 through siRNA-mediated silencing of specific IL-1 family receptors, antibody-mediated IL-36 receptor neutralisation, as well as through use of IL-36 receptor antagonist. We also investigated the pro-inflammatory activity of K53-truncated IL-37 *in vivo* by i.p. administration of this cytokine into wild type versus *IL-36R*$^{-/-}$ animals.

Reagents and antibodies

Anti-IL-37 mouse monoclonal antibody (catalog #60296-1-Ig) was obtained from Proteintech (Rosemont, IL, USA). Anti-hIL-36R neutralizing antibody (catalog #MAB8721), anti-hIL-36α neutralizing antibody (catalog #AF1078-SP), anti-hIL-36β neutralizing antibody (catalog #AF1099-SP), anti-IL-1β (catalog #MAB201), anti-IL-1RAcP (catalog #AF676), anti-IL-36R (catalog #AF872) and anti-SIGIRR (catalog #AF990) antibodies were obtained from R&D Systems (Minneapolis, MN, USA). Anti-IL-36γ neutralizing antibody (catalog #24723-1-AP) was obtained from Proteintech (Rosemont, IL, USA). Anti-MyD88 antibody (catalog #ab2064) was obtained from Abcam (Cambridge, UK). Anti-IκBα (catalog #9242s), anti-phospho-NFkB-p65 (catalog #3033p), anti-p38 MAPK (catalog #9212s), anti-phospho-p38 MAPK (catalog #4511s) and anti-MEK (catalog #9122) antibodies were obtained from Cell Signaling Technology (Danvers, MA, USA). Anti-actin antibody (catalog #0869100-CF) was obtained from MP Biomedicals (Irvine, CA, USA). Peroxidase AffiniPure anti-mouse (catalog #115-035-003), anti-rabbit (catalog #111-035-003) and anti-goat (catalog #705-035-003) secondary antibodies were obtained from Jackson ImmunoResearch Laboratories (West Grove, PA, USA). Purified neutrophil-derived cathepsin G (catalog #219373) was purchased from Calbiochem/Merck Millipore (Burlington, MA, USA). Purified neutrophil-derived elastase (catalog #20927.01) was

purchased from Serva (Heidelberg, Germany). Polymyxin B sulfate solution (catalog #420413) was obtained from Calbiochem/Merck Millipore (Burlington, MA, USA).

Cell culture

HaCaT cells were cultured in RPMI-1640 media (Gibco) supplemented with 5% fetal calf serum (FCS). Primary human keratinocytes cells (catalog #FC-0007) were purchased from Cell Systems (Troisdorf, Germany) and cultured in DermaLife K fully supplemented keratinocyte growth medium (catalog #LM-0027). HeLa$^{IL\text{-}36R}$ cell lines were generated by transfection with pCXN2.IL-1Rrp2 (IL-36R) plasmids followed by selection using G-418 antibiotic (Sigma), as described previously (*13*). HeLa and HeLa$^{IL\text{-}36R}$ cells were cultured in RPMI-1640 media (Gibco), supplemented with 5% FCS. Mouse embryonic fibroblast (MEF) and mouse 308 keratinocyte (308KC) cell lines were cultured in DMEM media (Gibco), supplemented with 10% FCS. All cells were cultured at 37°C in a humidified atmosphere with 5% CO_2.

Measurement of cytokines and chemokines

After treatment, cell culture supernatants were collected and clarified by centrifugation for 5 min 800 *g*. Cytokines and chemokines were measured from clarified cell culture supernatants using specific ELISA kits (catalog #DY206; #DY208; #DY214; #DY275; #DY360; #DY406; #DY410; #DY415; #DY452; #DY453; #DY760) obtained from R&D Systems (Minneapolis, MN, USA). Each assay was repeated a minimum of three times and all cytokine assays were carried out using triplicate samples from each culture.

Expression and purification of recombinant proteins

Truncated IL-1α (active IL-1α) was expressed in BL21 ClearColi bacteria purchased from Lucigen, (Middleton, WI, USA; catalog #60810-1) and purified as described previously (*18*). Full-length IL-1β, IL-36β, IL-36RA and IL-37b proteins were generated by cloning the human coding sequences in-frame with the poly-histidine tag sequence in the bacterial expression vector pET45b. Individual clones were sequence-validated. Protein was expressed by addition of 100 µM isopropyl β-D-1-thiogalactopyranoside (IPTG) to exponentially growing cultures of BL21 ClearColi followed by incubation for 3 hr at 37°C. Bacteria were lysed by sonication, and poly-histidine tagged proteins were captured using nickel-nitrilotriacetic acid agarose (NiNTA) beads (purchased from Expedeon, San Diego, USA; catalog #ab270549), followed by elution into PBS (pH 7.2) in the presence of 100 mM imidazole. All recombinant cytokines were frozen in elution buffer at -70°C immediately after purification. For IL-1β purification,

sodium sarkosyl was added to the bacterial lysate to a final volume of 0.25%. Bacteria were lysed by sonication and sarkosyl was subsequently sequestered by addition of TritonX-100 to a final volume of 0.5% and captured using nickel-NTA agarose followed by elution, as above. Truncations of IL-37 that included a caspase-3-processing motif (DEVD) were generated by cloning the DEVD-modified cytokine coding sequence in frame with the poly-histidine tag sequence in the bacterial expression vector pET45b, as described previously (*40*). All IL-37 mutants were expressed and purified in the same way and were immediately frozen at -70 ºC after elution into PBS (pH 7.2) in the presence of 100 mM imidazole. Recombinant poly-histidine-tagged caspase-1 and caspase-3 were expressed in LPS-free strain BL21 ClearColi bacteria and purified as described previously (*41*). Recombinant human cathepsin S was expressed in yeast *P. pastoris* and purified as described previously (*42*).

Purification of primary human neutrophils and preparation of neutrophil degranulates

Primary human neutrophils were purified from donor blood using the plasma-Percoll gradient method as described previously (*13*). To prepare degranulates, neutrophils (10^7 cells per treatment) were stimulated in the presence or absence of 100 nM PMA in Hank's balanced salt solution (HBSS)/0.25% BSA for 2 h at 37°C in a humidified atmosphere with 5% CO_2. Supernatants were harvested and clarified by centrifugation and stored at −80°C before use in protease cleavage assays.

Activation of cytokines by proteolysis and assessment of bioactivity

Proteolysis reactions (40–100 µL final volume) were carried out in protease reaction buffer (50 mM HEPES [pH 7.4], 75 mM NaCl, 0.1% CHAPS) for 2 h at 37°C. For IL-1β and IL-36 cytokine bioassays, cytokines were typically cleaved at 50-100 nM and subsequently diluted onto target cells at a final concentration of 1-2 nM. For IL-37 cytokine bioassays, IL-37 cytokines were typically cleaved at 500 nM and subsequently diluted onto target cells at a final concentration of 20 nM. It is important to note that IL-37 cytokine preparations appeared to be much more unstable than IL-36 family cytokines and, consequently, the bioactivity of IL-37 cytokines was assessed immediately after proteolysis. For preparation of truncated versions of IL-37, recombinant purified caspase-3 (~50 nM) prepared in LPS-free ClearColi bacteria was added to DEVD-modified IL-37 truncations (500 nM) in 100 µl reactions, followed by incubation for 1 h at 37°C. Due to the labile nature of recombinant IL-37 cytokine preparations, as noted above, truncated IL-37 cytokines were used immediately upon cleavage and compared with buffer controls containing identical amounts of recombinant caspase-3. For experiments

involving IL-36Ra, anti-IL-36R neutralizing antibodies or anti-IL-36 family cytokine neutralizing antibodies, cells were pre-incubated for 1h at 37°C with IL-36Ra (100 nM), or with neutralizing antibodies (2 μg/ml) for various times as indicated in the figure legends, before treatment of cells with cleavage reaction products described above.

Western immunoblotting

Protein samples were prepared using SDS/PAGE loading buffer (2 % SDS, 50 mM Tris-HCl, pH 6.8, 10 % glycerol, 2.5 % β-mercaptoethanol), boiled for 7 min and electrophoresed on 12-13.5 % SDS-PAGE gels. Proteins were then transferred onto nitrocellulose membranes at 40 mA, overnight. Membranes were blocked for 1 h (in 5 % NFDM, 0.05 % sodium azide in Tris-buffered saline, Tween-20, TBST). The indicated proteins were probed using specific antibodies, typically diluted 1:2000. Membranes were washed 3 times in TBST and then incubated with the relevant HRP-conjugated secondary antibody diluted 1:2000. Membranes were again washed and proteins were visualized with SuperSignal West Pico (ThermoFisher Scientific, Waltham, MA, USA) and exposure to autoradiography films.

Coupled In Vitro Transcription/Translation Reactions

In vitro transcription/translation reactions were carried out using 1 μg of purified plasmid template added to a rabbit reticulocyte lysate system (Promega, UK) for 1 h at 30 °C. Briefly, 1 μg of pET45.IL-37 expression plasmid was incubated for 1 h at 30°C in a total volume of 50 μl containing T7 polymerase, 1 μl of translation grade ^{35S}methionine (1000, μCi/ml; Amersham), 50% rabbit reticulocyte lysate, RNAsin and an amino acid mixture lacking methionine. Reaction products were then aliquoted and stored at -70°C until required. ^{35S}-labeled IL-37 was included in proteolysis reactions and reactions were then analysed by SDS-PAGE, followed by fluorography.

RNA interference

HaCaT cells (10^6) were nucleofected with 2 μM of each siRNA (see sequences below), in nucleofection buffer (5 mM KCl, 15 mM $MgCl_2$, 20 mM HEPES, 150 mM Na_2HPO_4 [pH 7.2]) using Amaxa Nucleofector (Program U020). Cells were plated in 6-well plates (4 x 10^5 cells/well) or in 24-well plates (1 x 10^5 cells/well) and 48 h after nucleofection cells were stimulated as indicated.

Control siRNA sense oligo: 5'-UAAGGCUAUGAAGAGAUAC-3'

IL-36R siRNA sense oligo #1: 5'-GCCAGAGUCAAUUCAGUACAU-3'

IL-36R siRNA sense oligo #2: 5'-CGACAUUGUUCUUUGGUAU-3'
IL-1RAcP siRNA sense oligo #1: 5'-GAUGAAACAAGAACUCAGA-3'
IL-1RAcP siRNA sense oligo #2: 5'-CAGCCAAGGUGAAGCAGAA-3'
SIGIRR siRNA sense oligo #1: 5'-CCGCCGACCUCUUGGUGAA-3'
SIGIRR siRNA sense oligo #2: 5'-GCUGAUUCUUCGAGGCCGA-3'
MyD88 siRNA sense oligo #1: 5'-GGCACCUGUGUCUGGUCUA-3'
MyD88 siRNA sense oligo #2: 5'-GGGCAUCACCACACUUGAU-3'

Site-directed mutagenesis

Site-directed mutagenesis of IL-37 was carried out using the Q5 site-directed mutagenesis kit (catalog code #E0554S) obtained from New England Biolabs (Ipswich, MA, USA). PCR reactions were set up on a 25 µl scale comprised of Q5 HF master mix, 10 ng of template DNA per reaction and 500 nM primers. After the PCR step, 1 µl of PCR products were digested with KLD enzyme in a 10 µl reaction, followed by transforming 5 µl of the reaction into 50 µl of supercompetent *E. Coli* (DH5α). Bacterial colonies were selected for sequencing after overnight incubation and mutagenesis was verified by sequencing (Eurofins Genomics, Ebersburg, Germany).

N-Terminal sequencing experiments

IL-37 (4 µg) protein was incubated in the presence or absence of a titration of purified neutrophil elastase or purified cathepsin S for 2 h at 37°C. Reactions were subsequently electrophoresed on 15% Tris-tricine gels, stained with Coomassie brilliant blue and duplicate gels transferred to 0.2 µM SequiBlot PVDF membrane (catalog#1620184) obtained from Bio-Rad (Hercules, CA, USA). IL-37 cleavage products, as indicated, were excised under sterile conditions and sent for N-Terminal (Edman) degradation sequencing at Tufts University Core Facility (Boston, MA, USA).

PyMol analysis

Protein structural superimposition was performed with PyMol build-in "align" script with default settings using backbone carbon atoms. For structural comparison PDB deposited files used were: IL-1α - 2ILA; IL-18 - 3WO2; IL36γ - 4IZE; IL-37 - 5HN1.

RNA-Seq experiments

Primary human neonatal foreskin-derived keratinocytes (passage 3) were used for gene expression analysis. Primary keratinocytes (10^6/well) were left untreated or stimulated with active IL-36 (10 nM), active IL-37 (10 nM) or TNF (10 ng/ml). At 2 h and 4 h, supernatants and cells were harvested with RNAprotect cell reagent (QIAGEN) and immediately stored at −80°C. RNA sequencing analyses of samples was performed by IMGM Laboratories (Martinsried, Germany). One RNA sequencing library was prepared from the isolated RNA samples with the Illumina TruSeq® Stranded mRNA HT technology. This approach uses fragmentation, a poly-T oligo pulldown and sequencing adapter ligation. RNA sequencing was performed on the Illumina NextSeq® 500 next generation sequencing system and its high output mode with 1 x 75 bp single-read chemistry. Gene expression analysis and the generation of heatmaps was conducted using software available from http://www.chibi.ubc.ca/matrix2png/bin/matrix2png.cgi. Differentially expressed genes were identified relative to untreated control samples analysed at the same time.

Animal experiments

All animal protocols were approved by the Scientific Animal Protection Division of the Health Products Regulatory Authority of Ireland and Trinity College Ethics Committee (license number AE19136/P079). Ten-week-old wild type or IL36R$^{-/-}$ C57BL/6 mice (n=5-7/group) were injected intraperitoneally with the indicated doses of active K53-IL-37 or PBS in a total volume of 200 µl. Twenty-two hours later animals were sacrificed by CO_2 inhalation. Peritoneal washes were performed by injecting 4 ml of ice-cold sterile PBS with 2 mM EDTA and aspirated using a syringe and 21G needle. Cells were centrifuged at 400 x g for 5 mins at 4ºC. Pellets were resuspended in FACS buffer (PBS, 2 mM EDTA, 2% FBS). Aliquots were taken and live cell numbers were determined by trypan blue exclusion assay. Cells were stained with a pre-defined panel of fluorescently labelled antibodies and a live-dead fixable stain. After fixation in PFA 2% for 20min on ice, cells were acquired in an LSR Fortessa equipped with 488, 633, 405 and 561 lasers and analysed using FlowJo Software according to the gating strategy in the supplementary figure. Total cell numbers for each cell type were calculated using the pre-determined total cell numbers in peritoneal washes and percentages determined by FACS.

Statistical Analysis

Error bars are represented as mean ± SEM. Statistical significance was calculated by Student's t test. Statistical tests were performed in Microsoft Excel using the TTEST function. For tests involving multiple comparisons that required post-hoc adjustment, Benjamini-Hochberg

procedure was employed, FDR discovered and adjusted p-values were calculated. Bar graphs were plotted as mean ± SDM and statistical significance was denoted as follows: *** = $p < 0.001$, ** = $p < 0.01$, * = $p < 0.05$. For in vivo experiments, statistical analysis was performed using Prism software and expressed as mean± SEM. Statistical significance was determined using One-way ANOVA and Dunette's post hoc test comparing all treated groups to PBS controls. *** = $p < 0.001$, ** = $p < 0.01$, * = $p < 0.05$.

SUPPLEMENTARY MATERIALS

Figures S1-S6

Data file S1

Reproducibility Checklist

REFERENCES AND NOTES

1. J.E. Sims, D.E. Smith, The IL-1 family: regulators of immunity. *Nat. Rev. Immunol.* **10**, 89-102 (2010).
2. S.J. Martin, Cell death and inflammation: the case for IL-1 family cytokines as the canonical DAMPs of the immune system. *FEBS J.* **283**, 2599-2615 (2016).
3. S. Kumar, P.C. McDonnell, R. Lehr, L. Tierney, M.N. Tzimas, D.E. Griswold, E.A. Capper, R. Tal-Singer, G.I. Wells, M.L. Doyle, P.R. Young, Identification and initial characterization of four novel members of the interleukin-1 family. *J Biol. Chem.* **275**, 10308-10314 (2000).
4. E. Dunn, J.E. Sims, M.J. Nicklin, L.A. O'Neill, Annotating genes with potential roles in the immune system: six new members of the IL-1 family. *Trends Immunol.* **22**, 533-536 (2001).
5. M.F. Nold, C.A. Nold-Petry, J.A. Zepp, B.E. Palmer, P. Bufler, C.A. Dinarello, IL-37 is a fundamental inhibitor of innate immunity. *Nat. Immunol.* **11**, 1014-1022 (2010).
6. C.A. Dinarello, C. Nold-Petry M. Nold, M. Fujita, S. Li, S. Kim, P. Bufler, Suppression of innate inflammation and immunity by interleukin family member interleukin-37. *Eur. J. Immunol.* **46**, 1067-1081 (2016).
7. G. Pan, P. Risser, W. Mao, D.T. Baldwin, A.W. Zhong, E. Filvaroff, D. Yansura, L. Lewis, C. Eigenbrot, W.J. Henzel, R. Vandlen, IL-1H, an interleukin 1-related protein that binds IL-18 receptor/IL-1Rrp. *Cytokine* **13**, 1-7 (2001).
8. C.A. Nold-Petry, C.Y. Lo, I. Rudloff, K.D. Elgass, S. Li, M.P. Gantier, A.S. Lotz-Havla, S.W. Gersting, S.X. Cho, J.C. Lao, A.M. Ellisdon, B. Rotter, T. Azam, N.E. Mangan, F.J. Rossello, J.C. Whisstock, P. Bufler, C. Garlanda, A. Mantovani, C.A. Dinarello, M.F. Nold, IL-37 requires the receptors IL-18Rα and IL-1R8 (SIGIRR) to carry out its multifaceted anti-inflammatory program upon innate signal transduction. *Nat. Immunol.* **16**, 354-365 (2015).
9. S. Sharma, N. Kulk, M.F. Nold, R. Gräf, S.H. Kim, D. Reinhardt, C.A. Dinarello, P. Bufler, The IL-1 Family Member 7b translocates to the nucleus and down-regulates proinflammatory cytokines. *J. Immunol.* **180**, 5477-5482 (2008).
10. I.S. Afonina, C. Müller, S.J. Martin, R. Beyaert, Proteolytic processing of interleukin-1 family cytokines: variations on a common theme. *Immunity* **42**, 991-1004 (2015).

11. D.J. Hazuda, J. Strickler, P. Simon, P.R. Young, Structure-function mapping of interleukin-1 precursors. Cleavage leads to a conformational change in the mature protein. *J. Biol. Chem.* **266**, 7081-7086 (1991). PMID: 2016316
12. N.A. Thornberry, H.G. Bull, J.R. Calaycay, K.T. Chapman, A.D. Howard, M.J. Kostura, D.K. Miller, S.M. Molineaux, J.R. Weidner, J. Aunins, K.O. Eliston, J.M. Ayala, F.J. Casano, J. Chin, G.J.F. Ding, L. A. Egger, E.P. Gaffney, G. Limjuco, O.C. Palyhat, S.M. Raju, A.M. Rolando, J.P. Salley, T.T. Yamin, T.D. Lee, J.E. Shively, M. MacCross, R.A. Mumford, J.A. Schmidt, M.J. Tocci, A novel heterodimeric cysteine protease is required for interleukin-1β processing in monocytes. *Nature* **356**, 768-774 (1992).
13. C.M. Henry, G.P. Sullivan, D.M. Clancy, I.S. Afonina, D. Kulms, S.J. Martin, Neutrophil-derived proteases escalate inflammation through activation of IL-36 family cytokines. *Cell Rep.* **14**, 708-722 (2016).
14. J.S. Ainscough, T. Macleod, D. McGonagle, R. Brakefield, J.M. Baron, A. Alase, M. Wittmann, M. Stacey, Cathepsin S is the major activator of the psoriasis-associated proinflammatory cytokine IL-36γ. *Proc. Natl. Acad. Sci.* **114**, E2748-E2757 (2017).
15. S. Kumar, C.R. Hanning, M.R. Brigham-Burke, D.J. Rieman, R. Lehr, S. Khandekar, R.B. Kirkpatrick, G.F. Scott, J.C. Lee, F.J. Lynch, W. Gao, A. Gambotto, M.T. Lotze, Interleukin-1F7b (IL-1H4/IL-1F7) is processed by caspase-1 and mature IL-1F7b binds to the IL-18 receptor but does not induce IFN-γ production. *Cytokine* **18**, 61-71 (2002).
16. A.M. Bulau, M.F. Nold, S. Li, C.A. Nold-Petry, M. Fink, A. Mansell, T. Schwerd, J. Hong, A. Rubartelli, C.A. Dinarello, P. Bufler, Role of caspase-1 in nuclear translocation of IL-37, release of the cytokine, and IL-37 inhibition of innate immune responses. *Proc. Natl. Acad. Sci.* **111**, 2650-2655 (2014).
17. S. Li, J. Amo-Aparicio, C.P. Neff, I.W. Tengesdal, T. Azam, B E. Palmer, R. López-Vales, P. Bufler, C.A. Dinarello, Role for nuclear interleukin-37 in the suppression of innate immunity. *Proc. Natl. Acad. Sci.* **116**, 4456-4461 (2019).
18. I.S. Afonina, G.A. Tynan, S.E. Logue, S.P. Cullen, M. Bots, A.U. Lüthi, E.P. Reeves, N.G. McElvaney, J.P. Medema, E.C. Lavelle, S.J. Martin, Granzyme B-dependent proteolysis acts as a switch to enhance the pro-inflammatory activity of IL-1α. *Mol. Cell* **44**, 265-278 (2011).
19. E. Lefrançais, S. Roga, V. Gautier, A. Gonzalez-de-Peredo, B. Monsarrat, J.P. Girard, C. Cayrol, IL-33 is processed into mature bioactive forms by neutrophil elastase and cathepsin G. *Proc. Natl. Acad. Sci.* **109**, 1673-1678 (2012).
20. D.M. Clancy, G.P. Sullivan, H.B.T. Moran, C.M. Henry, E.P. Reeves, N.G. McElvaney, E.C. Lavelle, S.J. Martin, Extracellular neutrophil proteases are efficient regulators of IL-1, IL-33, and IL-36 cytokine activity but poor effectors of microbial killing. *Cell Rep.* **22**, 2937-2950 (2018).
21. E. Kolaczkowska E, P. Kubes, Neutrophil recruitment and function in health and inflammation. *Nat. Rev. Immunol.* **13**, 159-175 (2013).
22. B. Korkmaz, M.S. Horwitz, D.E. Jenne, F. Gauthier, Neutrophil elastase, proteinase 3, and cathepsin G as therapeutic targets in human diseases. *Pharmacol. Rev.* **62**, 726-759 (2010).
23. G.P. Sullivan, C.M. Henry, D.M. Clancy, T. Mametnabiev, E. Belotcerkovskaya, P. Davidovich, S. Sura-Trueba, A.V. Garabadzhiu, S.J. Martin, Suppressing IL-36-driven inflammation using peptide pseudosubstrates for neutrophil proteases. *Cell Death Dis*, **9**, 378.
24. S. Li, C.P. Neff, K. Barber, J. Hong, Y. Luo, T. Azam, B.E. Palmer, M. Fujita, C. Garlanda, A. Mantovani, S. Kim, C.A. Dinarello, Extracellular forms of IL-37 inhibit innate inflammation in vitro and in vivo but require the IL-1 family decoy receptor IL-1R8. *Proc. Natl. Acad. Sci.* **112**, 2497-2502 (2015).
25. G. Pan, P. Risser, W. Mao, D.T. Baldwin, A.W. Zhong, E. Filvaroff, D. Yansura, L. Lewis, C. Eigenbrot, W.J. Henzel, R. Vandlen, IL-1H, an interleukin 1-related protein that binds IL-18 receptor/IL-1Rrp. *Cytokine*. **13**, 1-7 (2001).

26. S.J. Martin, V. Frezza, P. Davidovich, Z. Najda and D.M. Clancy. IL-1 family cytokines serve as 'activity recognition receptors' for aberrant protease activity indicative of danger. *Cytokine* **157,** 155935 (2022).
27. I.C. Scott, D.G. Rees and E.S. Cohen. New perspectives on IL-33 and IL-1 family cytokines as innate environmental sensors. *Biochem. Soc. Trans.* 46, 1345–1353 (2018).
28. C.N. LaRock, J. Todd, D.L. LaRock, J. Olson, A.J. O'Donoghue, A.A.B. Roberston, M.A. Cooper, H.M. Hoffman, V. Nizet, IL-1beta is an innate immune sensor of microbial preoteolysis, *Sci. Immunol.* 1 eaah3239 (2016).
29. C. Cayrol, A. Duval, P. Schmitt, S. Roga, M. Camus, A. Stella, O. Burlet-Schiltz, A. Gonzalez-de-Peredo, J.P. Girard, Environmental allergens induce allergic inflammation through proteolytic maturation of IL-33, *Nat. Immunol.* 19 (2018) 375–385. (2018).
30. T. Macleod, J.S. Ainscough, C. Hesse, S. Konzok, A. Braun, A.-L. Buhl, J. Wenzel, P. Bowyer, Y. Terao, S. Herrick, M. Wittmann, M. Stacey, The Proinflammatory Cytokine IL-36γ Is a Global Discriminator of Harmless Microbes and Invasive Pathogens within Epithelial Tissues, Cell Rep. 33 108515 (2020).
31. V. Frezza, Z. Najda, P. Davidovich, G.P. Sullivan, S.J. Martin. IL-1α and IL-36 Family Cytokines Can Undergo Processing and Activation by Diverse Allergen-Associated Proteases Frontiers in Immunology 13, doi: 10.3389/fimmu.2022.879029 (2022).
32. E. Lefrançais, A. Duval, S. Roga, E. Mirey, E. Espinosa, C. Cayrol, J.P. Girard. Central domain of IL-33 is cleaved by mast cell proteases for potent activation of group-2 innate lymphoid cells. *Proc. Natl. Acad. Sci.* **111,** 15502-7 (2014).
33. R.D.A. Wilkinson, R. Williams, C. J. Scott and Roberta E. Burden. Cathepsin S: therapeutic, diagnostic, and prognostic potential *Biol. Chem.* 396, 867–882 (2015).
34. A.M. Ellisdon, Nold-Petry CA, D'Andrea L, Cho SX, Lao JC, Rudloff I, et al. Homodimerization Attenuates the Anti-Inflammatory Activity of Interleukin-37. *Sci. Immunol.* (2017) 2(8):eaaj1548. doi: 10.1126/sciimmunol.aaj1548
35. Eisenmesser EZ, Gottschlich A, Redzic JS, Paukovich N, Nix JC, Azam T, et al. Interleukin-37 Monomer Is the Active Form for Reducing Innate Immunity. Proc Natl Acad Sci USA (2019) 116(12):5514–22. doi: 10.1073/pnas.1819672116
36. Coll-Miro M, Francos-Quijorna I, Santos-Nogueira E, et al. Beneficial effects of IL#37 after spinal cord injury in mice. Proc Natl Acad Sci USA. 2016;113:1411-1416
37. G. Cavalli, I.W. Tengesdal, M. Gresnigt, T. Nemkov, R.J.W. Arts, J. Domínguez-Andrés, et al. The Anti-Inflammatory Cytokine Interleukin-37 Is an Inhibitor of Trained Immunity. Cell Rep. 35(1):108955. doi: 10.1016/j.celrep.2021.108955 (2021).
38. D.E. Smith, The biological paths of IL-1 family members IL-18 and IL-33. J. Leukoc. Biol. 89, 383–392 (2011).
39. J. Rivers-Auty, M.J.D Daniels, I Colliver, D.L. Robertson, D. Brough. Redefining the ancestral origins of the interleukin-1 superfamily Nature communications 9, 1156 1-12 (2018).
40. D.M. Clancy, C.M. Henry, P.B. Davidovich, G.P. Sullivan, E. Belotcerkovskaya, S.J. Martin, Production of biologically active IL-36 family cytokines through insertion of N-terminal caspase cleavage motifs. *FEBS J.* **6**, 338-348 (2016).
41. J.G. Walsh, S.E. Logue, A.U. Lüthi, S.J. Martin, Caspase-1 promiscuity is counterbalanced by rapid inactivation of processed enzyme. *J. Biol. Chem.* 286, 32513-32524 (2011).
42. M. Mihelic, A. Dobersek, G. Guncar, D. Turk. Inhibitory fragment from the p41 form of invariant chain can regulate activity of cysteine cathepsins in antigen presentation. *J. Biol. Chem*. 283, 14453-60 (2008).

Acknowledgments: Funding: We thank Dr. Fiona Roche for help with generation of volcano plots. The Martin laboratory is supported by the Irish Research Council Advanced Laureate

programme (IRCLA/2019/133), The European Research Council Advanced Grant Programme (101020534, DESTRESS) and Science Foundation Ireland (14/IA/2622). The Lavelle laboratory acknowledges support from Science Foundation Ireland grants 12/1A/1421 and 19/FFP/6484. The Walsh Laboratory is supported by the National Children's Research Centre project grant C/18/8. The Turk laboratory was supported by a grant (P1-0140) from the Slovene Research Agency

Author contributions: G.P.S. designed and performed experiments, analyzed data, and generated figure panels. P.D. designed and performed experiments analyzed data and generated figure panels. D.M.C. performed initial pilot experiments. Z.N. conducted experiments. N.M.W., R.W.W. and A.G. conducted *in vivo* experiments and analyzed data with supervision and contributions from E.C.L. Y.E.H.S. and P.T.W. designed and conducted some of the in vivo experiments. B.T. prepared human cathepsin S and provided input on conducting the Cat S proteolysis experiments. S.J.M conceived the study, designed and analyzed experiments, supervised the study and wrote the manuscript.

Competing interests. The authors declare no competing interests.

Data and materials availability: All data are available in the main text or the supplementary materials. RNA-seq data are available in the GEO database under accession number: GSE214863.

FIGURE LEGENDS

Fig. 1. Interleukin-37 is processed and activated by neutrophil elastase. (**A**) HaCaT keratinocytes were incubated with full-length IL-37 or active IL-36β and cytokine concentrations in culture supernatants were determined by ELISA. (**B**) Full-length IL-37 (500 nM) was incubated for 2h with supernatants from unstimulated (Ctrl s/n) or PMA-activated primary human neutrophils (PMA s/n) and reaction products were incubated with HaCaT cells at a final IL-37 concentration of 20 nM. Active IL-36β (2 nM) was included as a positive control. Cytokine/chemokine release was determined as in (A). (**C** and **D**) Full-length IL-37 (500 nM) was incubated for 2 h with the indicated concentrations of purified human elastase, followed by assessment of IL-37 activity on HaCaT cells at a final IL-37 concentration of 20 nM (C) determined as in (A) and assessment of IL-37 proteolysis by SDS-PAGE analysis and western blotting (D). (**E** and **F**) Full-length IL-37 (500 nM) was incubated for 2 h with the indicated concentrations of purified human cathepsin G, followed by assessment of IL-37 activity (E) on HaCaT cells at a final IL-37 concentration of 20 nM determined as in (A) and assessment of IL-37 proteolysis by SDS-PAGE analysis and western blotting (F). (**G**) Full-length IL-37 (500 nM) was incubated for 2 h with the indicated concentrations of purified human elastase, followed by assessment of IL-37 activity on primary human keratinocytes at a final IL-37 concentration of 20 nM, determined as in (A). (**H**) Timecourse analysis of IL-37 processing by elastase, as assessed by immunoblot. (**I**) Elastase-processed IL-37 samples (indicated by arrows) were subjected to N-terminal sequencing and cleavage sites were identified. (**J**) Point mutations within IL-37 were generated at T42G, V46G, T42G/V46G or V113G using site-directed mutagenesis. The effects of the latter point mutations on elastase-mediated activation of IL-37, compared to wild-type (WT) IL-37, were determined using the HaCaT cell bioassay at a final IL-37 concentration of 20 nM as described in (C). (**K**) Equal amounts (500 nM) of either wild type IL-37 or a V113G IL-37 point mutant were incubated for 2 h with the indicated concentrations of elastase, followed by assessment of IL-37 bioactivity on HaCaT cells at a final IL-37 concentration of 20 nM. (**L**) Truncations of IL-37 were generated at M43, H47, S49 or S114 through insertion of a caspase-3 cleavage site motif (DEVD) upstream of the indicated amino acids. After purification of the recombinant DEVD-IL-37 fusion proteins, the specific truncations were generated by incubation with recombinant active caspase-3, as indicated (lower panels). The pro-inflammatory activity of the individual DEVD-IL-37 truncations (20 nM final concentration) was assessed before and after cleavage with caspase-3, as indicated. Results shown are representative of at least three independent experiments. Error bars represent the mean ±SEM of triplicate determinations from representative experiments. ND denotes not detected. Significance levels, *** = $P < 0.001$, ** = $p < 0.01$, * = $P < 0.05$, determined using student t-test.

Fig. 2. Cathepsin S can also produce a pro-inflammatory form of IL-37. (**A**) Full-length IL-37 (500 nM) was incubated with the indicated concentrations of cathepsin S followed by assessment of IL-37 activity (20 nM final concentration) on HaCaT cells by measuring the indicated cytokines by ELISA at 24 h. **(B)** Proteolytic processing of ^{35}S-labeled IL-37 after incubation with the indicated concentrations of either cathepsin S or elastase for 2 h at 37°C. (**C**) Comparison of full-length IL-37 processing over a range of concentrations of elastase (10, 5 and 2.5 nM) or cathepsin S (100, 50 and 25 nM), followed by analysis by SDS-PAGE/immunoblotting. (**D**) Cathepsin S-processed IL-37 (indicated by arrow) was subjected to N-terminal sequencing and cleavage sites were identified. (**E**) A cathepsin S-processing site mutant (V52G) IL-37 was generated by site directed mutagenesis and the ability of cathepsin S (50, 25, 12.5 nM) and elastase (5, 2.5, 1.25 nM) to process and activate 20 nM wild type IL-37 versus V52G IL-37 was determined by HaCaT bioassay. (**F**) Equimolar amounts of wild type IL-37 or V52G IL-37 mutant were incubated for 2 h at 37°C with the indicated concentrations of cathepsin S, followed by western immunoblotting. (**G**) Sequence conservation of elastase and

cathepsin S processing sites within IL-37. (**H**) A caspase-3 cleavage motif (DEVD) was inserted proximal to the Cat S processing site in IL-37 to generate a DEVD-K53-IL-37 fusion protein. (**I, J**) Processing of WT versus DEVD-K53-IL-37 by caspase-3 or elastase was assessed by immunoblotting. (**K**) The pro-inflammatory activity of 20 nM DEVD-K53-IL-37 was assessed by bioassay on HaCaT cells, before and after cleavage by purified recombinant caspase-3 (1:20, 1:40, 1:80, 1:160 dilution of stock), as indicated. (**L**) The pro-inflammatory activity of wild type IL-37 (50, 25, 12.5 nM) versus DEVD-K53-IL-37 (50, 25, 12.5 nM) was assessed by bioassay on HaCaT cells, before and after cleavage by purified recombinant caspase-3 (1:50 dilution of stock), as indicated. Results shown are representative of at least three independent experiments. Error bars represent the mean ±SEM of triplicate determinations from representative experiments. ND denotes not detected.

Fig. 3. Mature IL-37 generates a robust pro-inflammatory signature similar to IL-36
(**A** and **B**) Full-length IL-1β (2 nM) was incubated with purified human caspase-1, elastase or cathepsin S, at the indicated concentrations, and processing/activation analyzed by immunoblot (A) and bioassay on HaCaT cells (B). (**C** and **D**) Full-length IL-37 (20 nM) was incubated with purified human caspase-1, elastase and cathepsin S, as in (A) and analyzed for processing/activity as in (A) and (B). (**E** and **F**) Primary human keratinocytes were treated with active IL-36β (2 nM) or active K53-IL-37 (20 nM) and differential gene expression determined by RNA-seq analysis was visualized by DGE heatmap (E) and volcano scatterplot (F). (**G**) Timecourse analysis of HaCaT cells treated with active 2 nM IL-36 (actIL-36) or 20 nM active K53-IL-37 and analyzed for NFκB pathway activation by immunoblotting for the indicated proteins. (**H**) Primary human keratinocytes were treated as in (E) and pro-inflammatory cytokine and chemokine concentrations in cell culture supernatants determined by ELISA. Results shown are representative of at least three independent experiments. Error bars represent the mean ±SEM of triplicate determinations from representative experiments. ND denotes not detected.

Fig. 4. Active IL-37 promotes inflammation in an IL-36 receptor-dependent manner
(**A**) Sequence alignment followed by structural superposition using PyMOL was performed for IL-37 (blue) compared with IL-36γ (red), IL-18 (green), IL-1α (yellow) and structural deviation values determined (RMSD). (**B**) DEVD-K53-IL-37 (20 nM) was incubated in the presence or absence of caspase-3 (1:50 of stock) and reactions used to treat primary human keratinocytes in the presence or absence of 100 nM hIL-36 receptor antagonist (IL-36Ra) for 24h, followed by determination of cytokine/chemokine concentrations in culture supernatants by ELISA. (**C**) Full-length IL-37 (20 nM) was incubated in the presence or absence of elastase, cathepsin S or cathepsin G and reactions used to treat HeLa wild-type (WT) or HeLa cells stably expressing IL-36 receptor (IL-36R). After 24h, culture supernatants were analyzed as above. (**D** to **F**) HaCaT cells were nucleofected with the indicated siRNAs and, 48 h later, cells were either untreated or treated with (D) 20 nM active K53-IL-37, 2 nM active IL-36β (activated with Cat G) or (E) 2 nM active IL-1α (act.IL-1α). Culture supernatants were analyzed, as above, and to confirm gene silencing, cell lysates were prepared from cells treated in (D) and immunoblotted for the indicated proteins. (**G**) HaCaT cells were incubated with active IL-36β (0.2 nM) in the presence or absence of a titration of active K53-IL-37. After 18h, cytokine/chemokine concentrations in culture supernatants were determined as above. Results shown are representative of three independent experiments. Error bars represent the mean ±SEM of triplicate determinations from representative experiments. ND denotes not detected.

Fig. 5. IL-37 pro-inflammatory activity is independent of IL-36 family cytokines
(**A**) HaCaT cells were incubated with mature active K53-IL-37 or mature IL-36γ, as indicated, in the presence or absence of anti-IL-36R-neutralizing antibodies (2 μg/ml final concentration) that

were added to cells either prior to addition of cytokines (T0) or at 90 or 180 min after addition of cytokines, as indicated. After 18 h cytokine concentrations in cell culture supernatants were determined by ELISA. (**B**-**D**) HaCaT cells were incubated with mature active K53-IL-37 or mature IL-36α, IL-36β or IL-36γ, as indicated, in the presence or absence of specific neutralizing antibodies (2 μg/ml final concentration) against IL-36α (B), IL-36β (C) or IL-36γ (D), followed by measurement of cytokine concentrations in cell culture supernatants at 18h, determined by ELISA. Recombinant forms of the indicated IL-36 cytokines served as positive controls. (**E**) HaCaT cells were incubated with mature active K53-IL-37 or mature IL-36γ, as indicated, in the presence or absence of anti-IL-36γ-neutralizing antibodies (8 μg/ml final concentration) that were added to cells either prior to addition of cytokines (T0) or at 60 or 120 min after addition of cytokines, as indicated. After 18 h cytokine concentrations in cell culture supernatants were determined by ELISA. Results shown are representative of three independent experiments. Error bars represent the mean ±SEM of triplicate determinations from representative experiments. ND denotes not detected.

Fig. 6. Mature IL-37 promotes inflammation on murine cells in vitro and in vivo.
(**A** and **B**) DEVD-K53-IL-37 (20 nM) was incubated in the presence or absence of caspase-3 (1:50 dilution of stock) and reactions used to treat (A) mouse embryonic fibroblasts (MEF) or (B) murine keratinocyte (308KC) cells, in the presence or absence of polymyxin B (10 μg/ml). After 14h, cytokine and chemokine concentrations in culture supernatants were determined by ELISA. (**C**) DEVD-K53-IL-37 was incubated in the presence or absence of caspase-3 as in (A), followed by analysis by immunoblot. (**D** and **E**) 10-week-old C57BL/6 female mice (n=5/group) were injected intraperitoneally with the indicated concentrations of active K53-IL-37 or PBS. After 24h, animals were sacrificed, peritoneal washes performed, cells harvested, and cell pellets resuspended in FACS buffer. Aliquots were then used to determine live cell numbers by trypan blue exclusion. Total cell numbers for each cell type were calculated using the pre-determined total cell numbers in peritoneal washes and percentages determined by FACS. Immune cell recruitment to the peritoneal cavity was determined by flow cytometry using antibodies specific for neutrophils, eosinophils and macrophages. (**F**) At the same timepoint, cytokine/chemokine concentrations from peritoneal lavages were determined by ELISA. Results shown are representative of two independent experiments. Error bars represent the mean ±SEM of triplicate determinations from representative experiments. Significance levels, *** = $P < 0.01$, ** =$p<0.05$, determined using One-way ANOVA and Dunette's post hoc test comparing all treated groups to PBS controls.

Fig. 7. IL-37-driven inflammation is partially abrogated in *IL-36R*$^{-/-}$ mice.
(**A** and **B**) Ten-week-old C57BL/6 wild-type (WT) or IL-36R null (KO) mice (n=5-7/group,) were injected intraperitoneally with active K53-IL-37 (10 μg per mouse, 4 female, 3 male) or PBS (3 female, 2 male). After 24 h, animals were sacrificed, peritoneal cells harvested and total cell numbers for each cell type were determined by flow cytometry using antibodies specific for neutrophils and macrophages (B). (**C**) At the same timepoint, cytokine and chemokine concentrations from peritoneal lavages were determined by ELISA. Results shown are representative of two independent experiments. Error bars represent the mean ±SEM of triplicate determinations from representative experiments. Significance levels, *** = $P < 0.01$, ** =$p<0.05$, *= $P < 0.1$, determined using One-way ANOVA and Dunette's post hoc test comparing all treated groups to PBS controls.

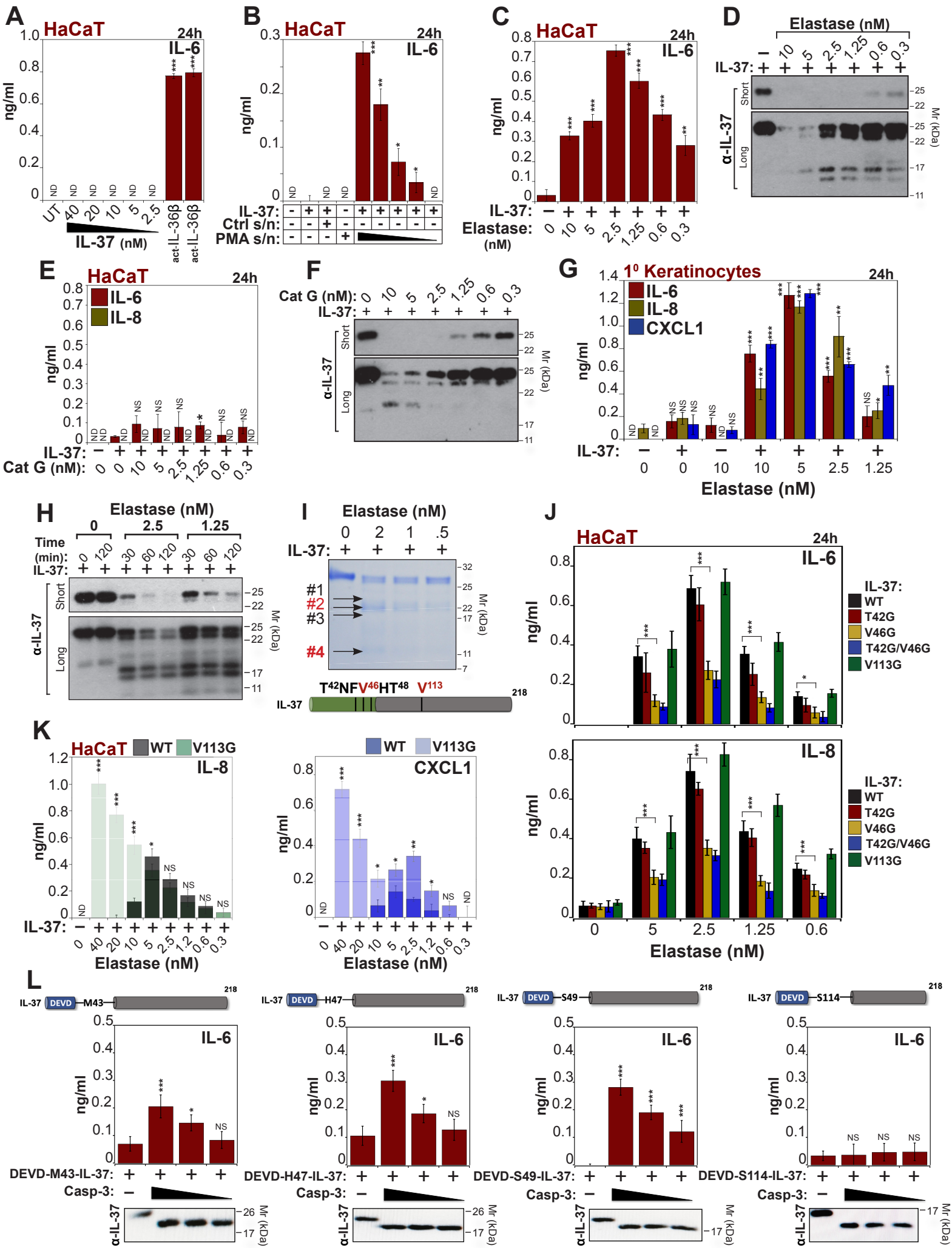
A
HaCaT
24h
IL-6
ng/ml
IL-37 (nM)
act-IL-36β
B
HaCaT
24h
IL-6
IL-37:
Ctrl s/n:
PMA s/n:
C
HaCaT
24h
IL-6
IL-37:
Elastase: (nM)
D
Elastase (nM)
IL-37:
α-IL-37
Short
Long
Mr (kDa)
E
HaCaT
24h
IL-6
IL-8
IL-37:
Cat G (nM):
F
Cat G (nM):
IL-37:
α-IL-37
G
1⁰ Keratinocytes
24h
IL-6
IL-8
CXCL1
IL-37:
Elastase (nM)
H
Elastase (nM)
Time (min):
IL-37:
α-IL-37
I
Elastase (nM)
IL-37:
#1
#2
#3
#4
T42NFV46HT48 V113
IL-37
J
HaCaT
24h
IL-6
IL-8
IL-37:
WT
T42G
V46G
T42G/V46G
V113G
ng/ml
Elastase (nM)
K
HaCaT
WT
V113G
IL-8
CXCL1
ng/ml
IL-37:
Elastase (nM)
L
IL-37
DEVD
M43
H47
S49
S114
IL-6
ng/ml
DEVD-M43-IL-37:
DEVD-H47-IL-37:
DEVD-S49-IL-37:
DEVD-S114-IL-37:
Casp-3:
α-IL-37
Mr (kDa)

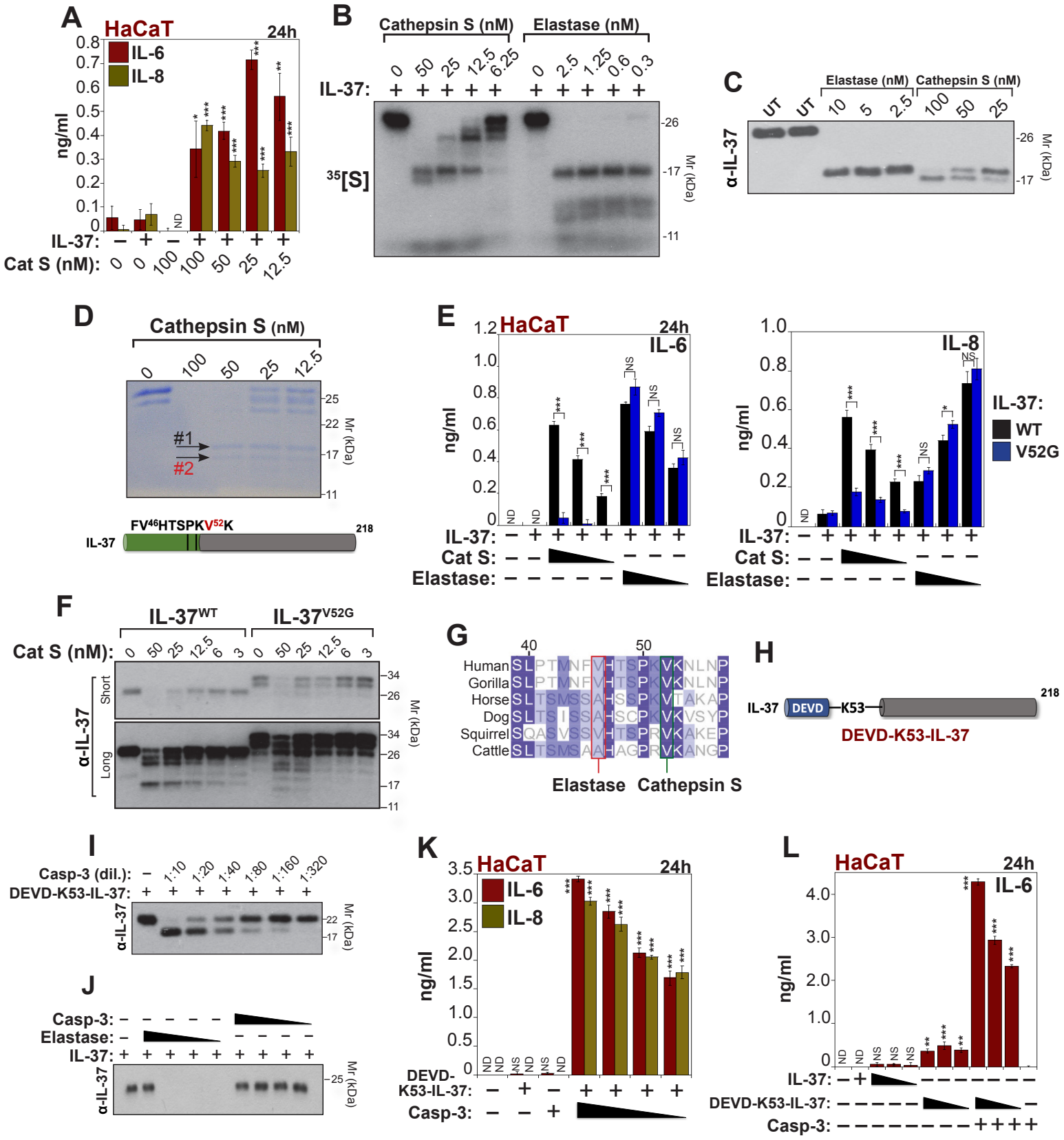
A
HaCaT
24h
IL-6
IL-8
ng/ml
IL-37:
Cat S (nM):
B
Cathepsin S (nM)
Elastase (nM)
IL-37:
35[S]
Mr (kDa)
C
Elastase (nM)
Cathepsin S (nM)
UT
α-IL-37
Mr (kDa)
D
Cathepsin S (nM)
#1
#2
Mr (kDa)
FV46HTSPKV52K
IL-37
218
E
HaCaT
24h
IL-6
IL-8
ng/ml
IL-37:
WT
V52G
Cat S:
Elastase:
F
IL-37WT
IL-37V52G
Cat S (nM):
Short
Long
α-IL-37
Mr (kDa)
G
Human
Gorilla
Horse
Dog
Squirrel
Cattle
Elastase
Cathepsin S
H
IL-37
DEVD
K53
218
DEVD-K53-IL-37
I
Casp-3 (dil.):
DEVD-K53-IL-37:
α-IL-37
Mr (kDa)
J
Casp-3:
Elastase:
IL-37:
α-IL-37
Mr (kDa)
K
HaCaT
24h
IL-6
IL-8
ng/ml
DEVD-K53-IL-37:
Casp-3:
L
HaCaT
24h
IL-6
ng/ml
IL-37:
DEVD-K53-IL-37:
Casp-3:

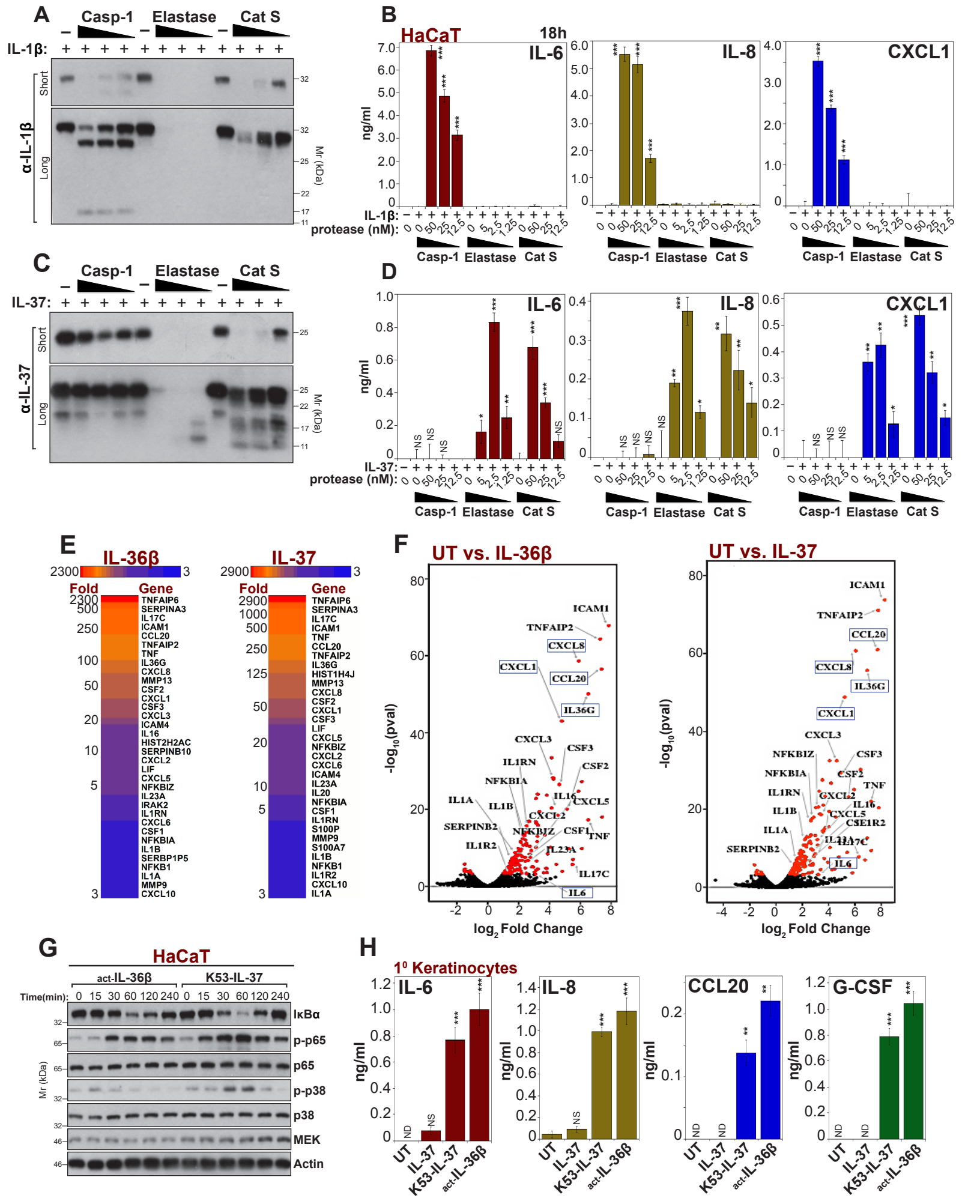
A
Casp-1
Elastase
Cat S
IL-1β:
α-IL-1β
Short
Long
Mr (kDa)
B
HaCaT
18h
IL-6
IL-8
CXCL1
ng/ml
IL-1β:
protease (nM):
Casp-1
Elastase
Cat S
C
IL-37:
α-IL-37
D
E
IL-36β
IL-37
Fold
Gene
F
UT vs. IL-36β
UT vs. IL-37
-log10(pval)
log2 Fold Change
G
HaCaT
act-IL-36β
K53-IL-37
Time(min):
IκBα
p-p65
p65
p-p38
p38
MEK
Actin
H
1⁰ Keratinocytes
IL-6
IL-8
CCL20
G-CSF
UT
IL-37
K53-IL-37
act-IL-36β

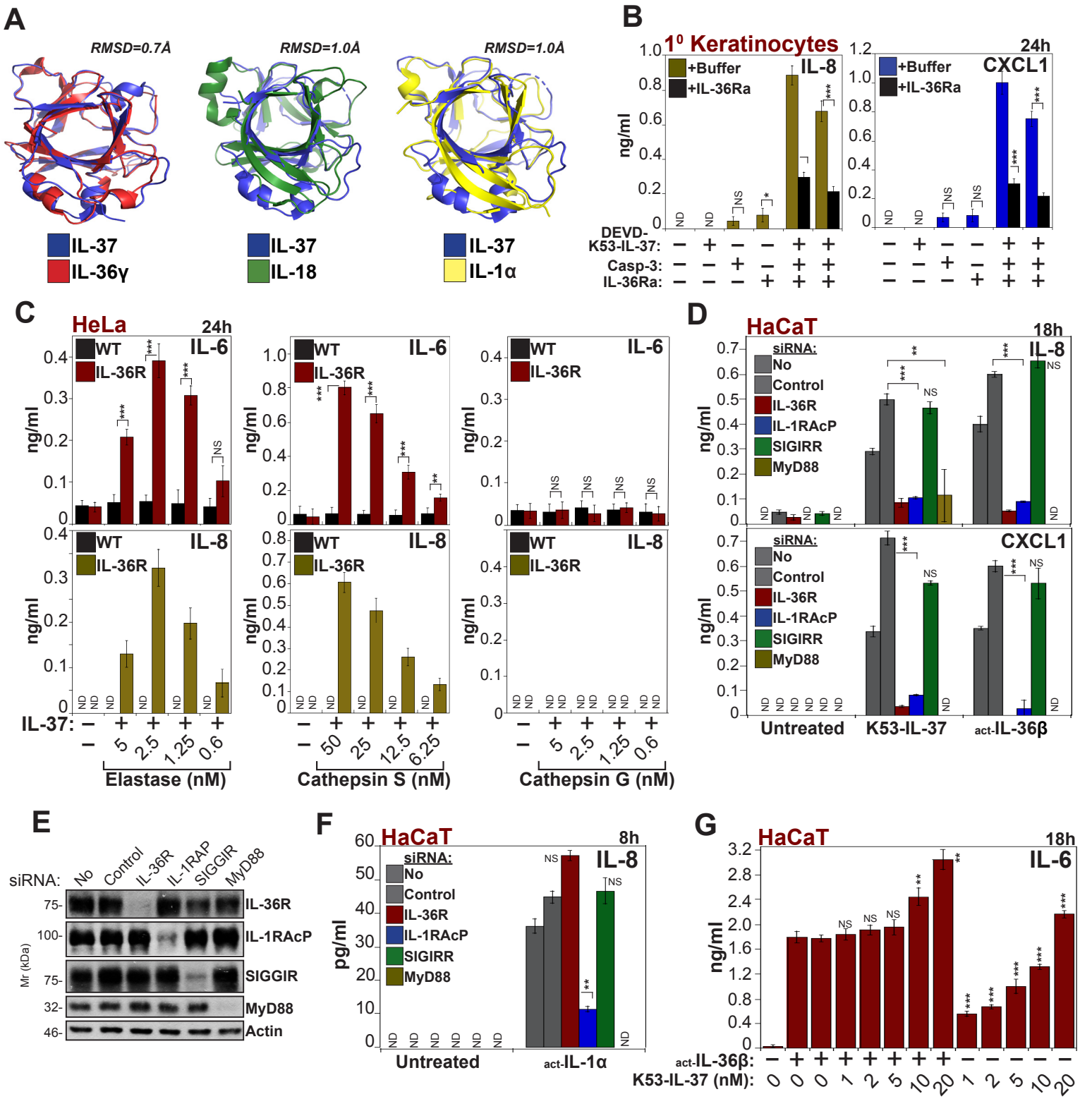
A
RMSD=0.7Å
RMSD=1.0Å
RMSD=1.0Å
IL-37
IL-36γ
IL-37
IL-18
IL-37
IL-1α
B
1⁰ Keratinocytes
+Buffer
+IL-36Ra
IL-8
CXCL1
24h
ng/ml
DEVD-K53-IL-37:
Casp-3:
IL-36Ra:
C
HeLa
24h
WT
IL-36R
IL-6
IL-8
ng/ml
IL-37:
Elastase (nM)
Cathepsin S (nM)
Cathepsin G (nM)
D
HaCaT
18h
siRNA:
No
Control
IL-36R
IL-1RAcP
SIGIRR
MyD88
IL-8
CXCL1
Untreated
K53-IL-37
act-IL-36β
E
siRNA:
No
Control
IL-36R
IL-1RAP
SIGGIR
MyD88
Mr (kDa)
75-
100-
75-
32-
46-
IL-36R
IL-1RAcP
SIGGIR
MyD88
Actin
F
HaCaT
8h
IL-8
pg/ml
Untreated
act-IL-1α
G
HaCaT
18h
IL-6
ng/ml
act-IL-36β:
K53-IL-37 (nM):

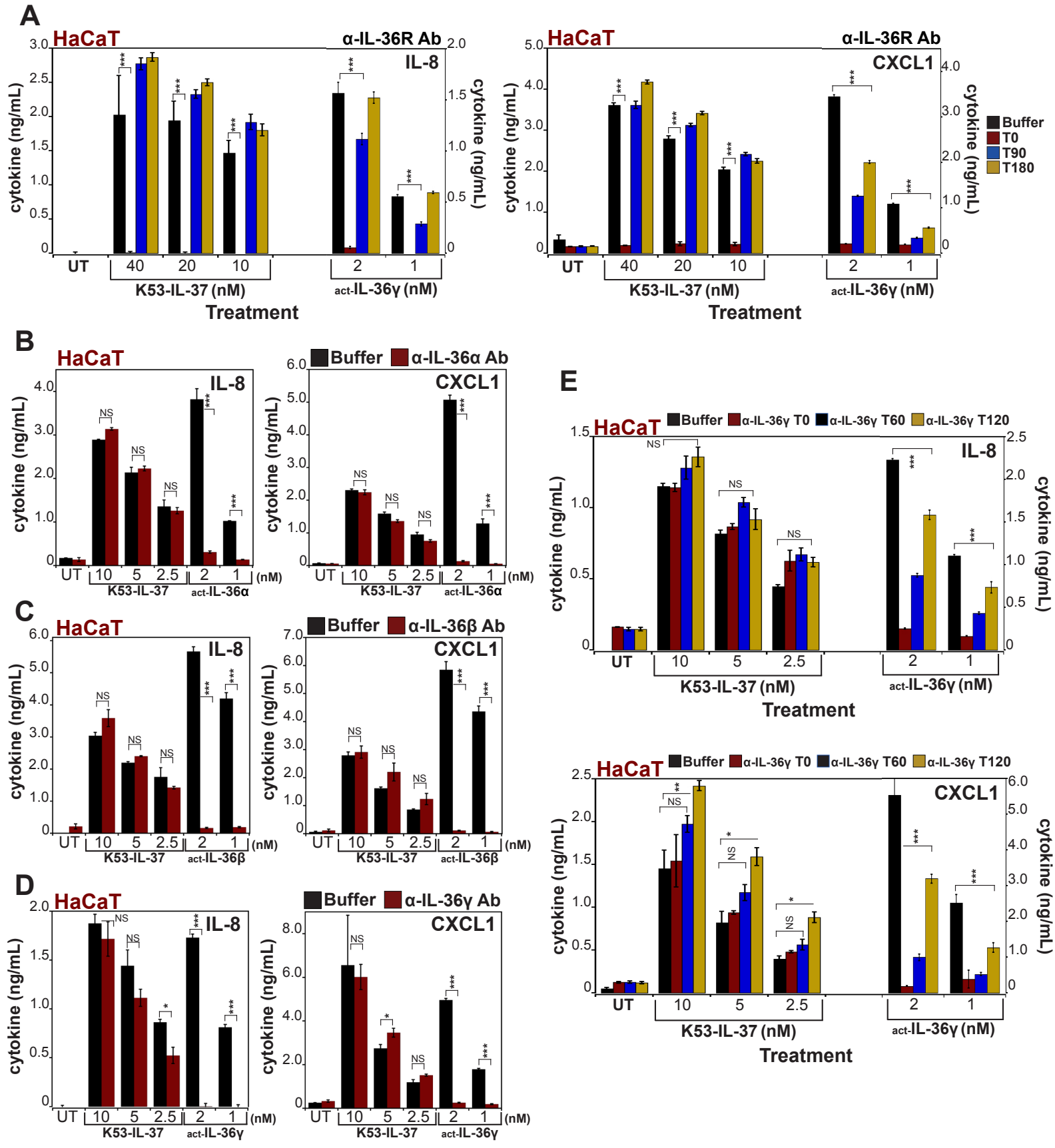
A
HaCaT
α-IL-36R Ab
IL-8
CXCL1
cytokine (ng/mL)
Buffer
T0
T90
T180
UT
40
20
10
2
1
K53-IL-37 (nM)
act-IL-36γ (nM)
Treatment
B
HaCaT
Buffer
α-IL-36α Ab
IL-8
CXCL1
NS
10
5
2.5
K53-IL-37
act-IL-36α
(nM)
C
HaCaT
Buffer
α-IL-36β Ab
IL-8
CXCL1
act-IL-36β
D
HaCaT
Buffer
α-IL-36γ Ab
IL-8
CXCL1
act-IL-36γ
E
HaCaT
Buffer
α-IL-36γ T0
α-IL-36γ T60
α-IL-36γ T120
IL-8
CXCL1

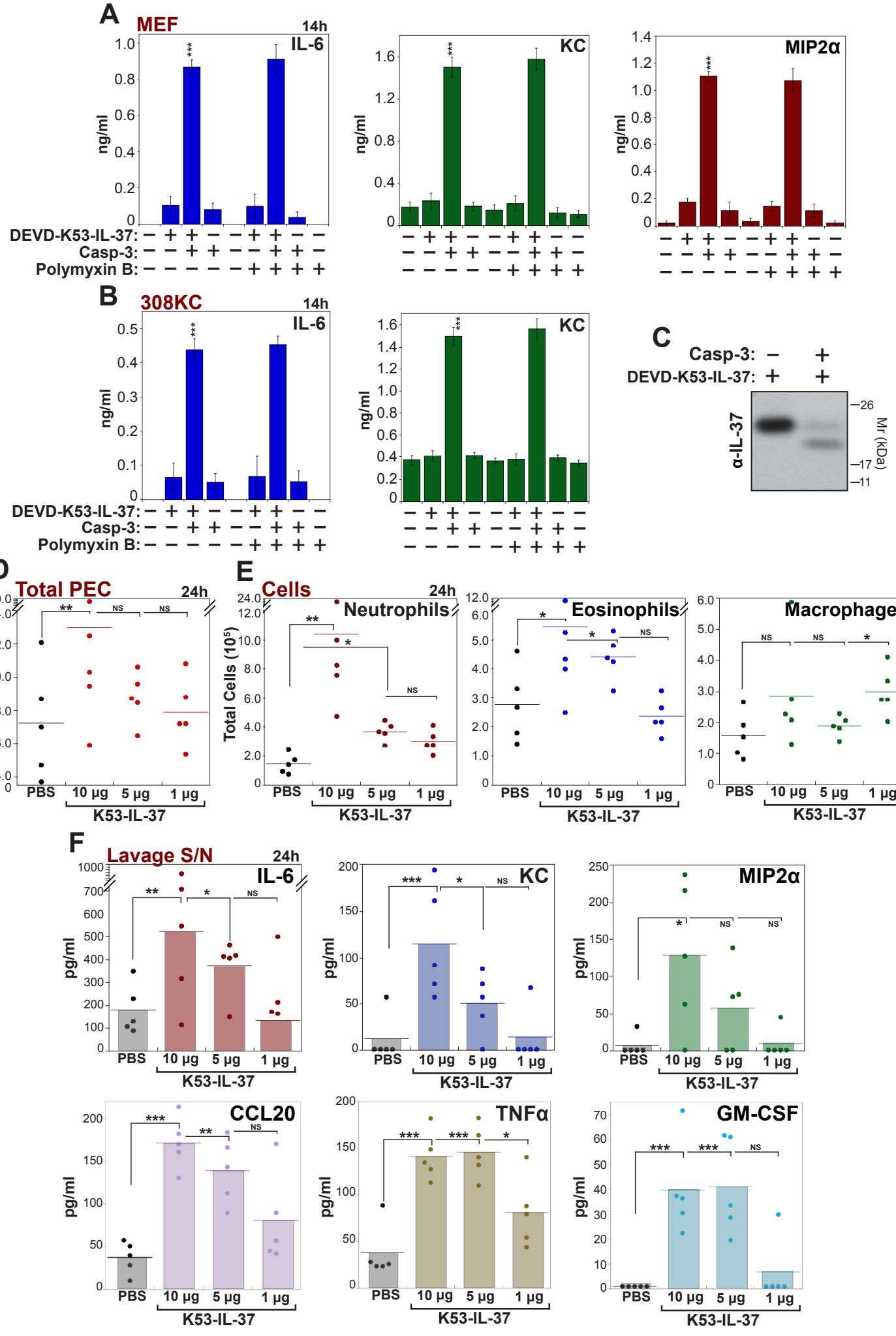
A
MEF
14h
IL-6
KC
MIP2α
ng/ml
DEVD-K53-IL-37:
Casp-3:
Polymyxin B:
B
308KC
14h
IL-6
KC
ng/ml
DEVD-K53-IL-37:
Casp-3:
Polymyxin B:
C
Casp-3:
DEVD-K53-IL-37:
α-IL-37
Mr (kDa)
26
17
11
D
Total PEC
24h
Total Cells (10⁶)
PBS
10 μg
5 μg
1 μg
K53-IL-37
NS
E
Cells
24h
Neutrophils
Eosinophils
Macrophages
Total Cells (10⁵)
F
Lavage S/N
24h
IL-6
KC
MIP2α
CCL20
TNFα
GM-CSF
pg/ml

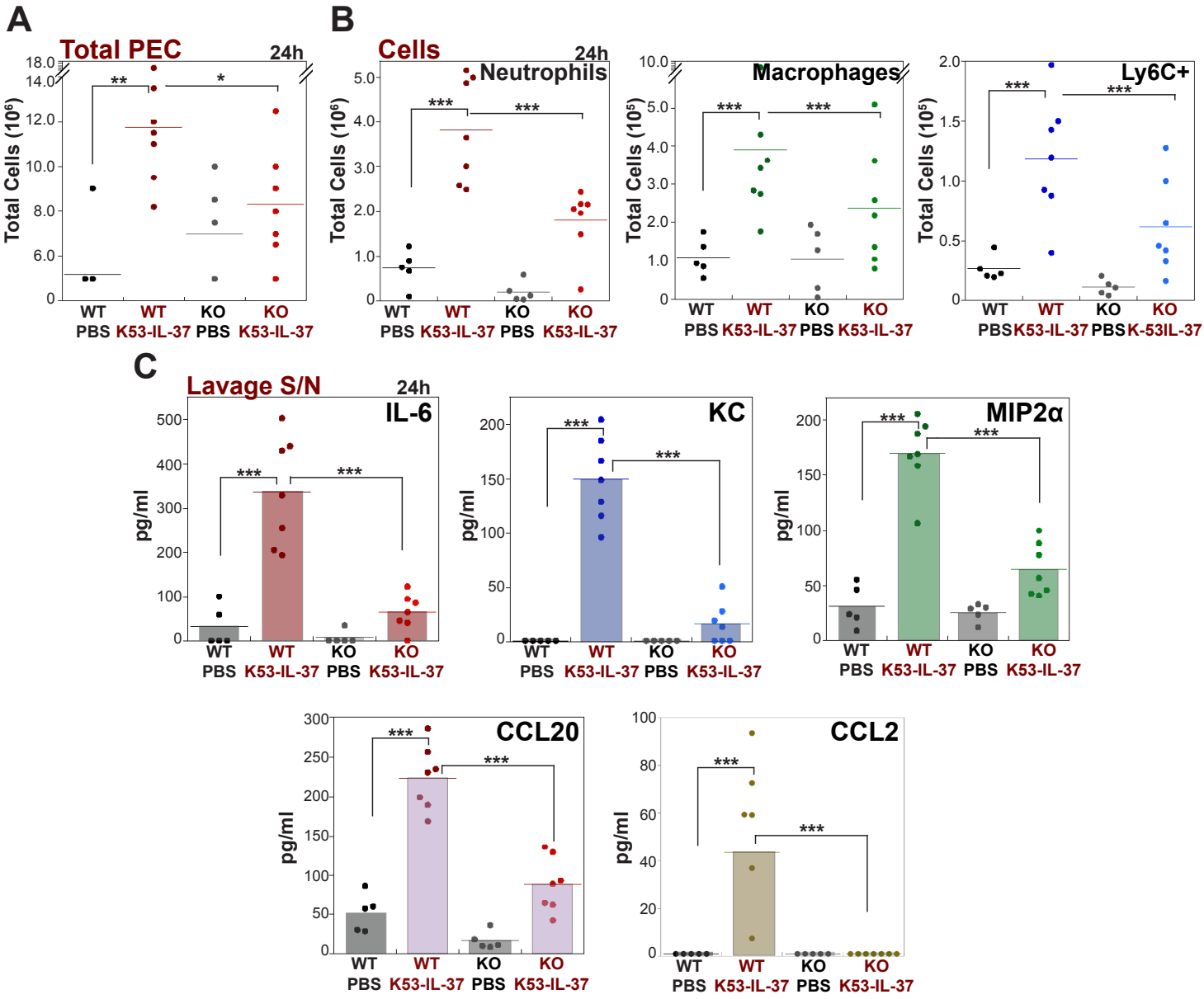
A
Total PEC
24h
Total Cells (10⁶)
18.0
14.0
12.0
10.0
8.0
6.0
0
**
*
WT PBS
WT K53-IL-37
KO PBS
KO K53-IL-37
B
Cells
24h
Neutrophils
Total Cells (10⁶)
5.0
4.0
3.0
2.0
1.0
0
***
***
Macrophages
Total Cells (10⁵)
10.0
5.0
4.0
3.0
2.0
1.0
0
Ly6C+
Total Cells (10⁵)
2.0
1.5
1.0
0.5
0
K-53IL-37
C
Lavage S/N
24h
IL-6
pg/ml
500
400
300
200
100
0
KC
200
150
100
50
0
MIP2α
CCL20
300
250
200
150
100
50
0
CCL2
100
80
60
40
20
0

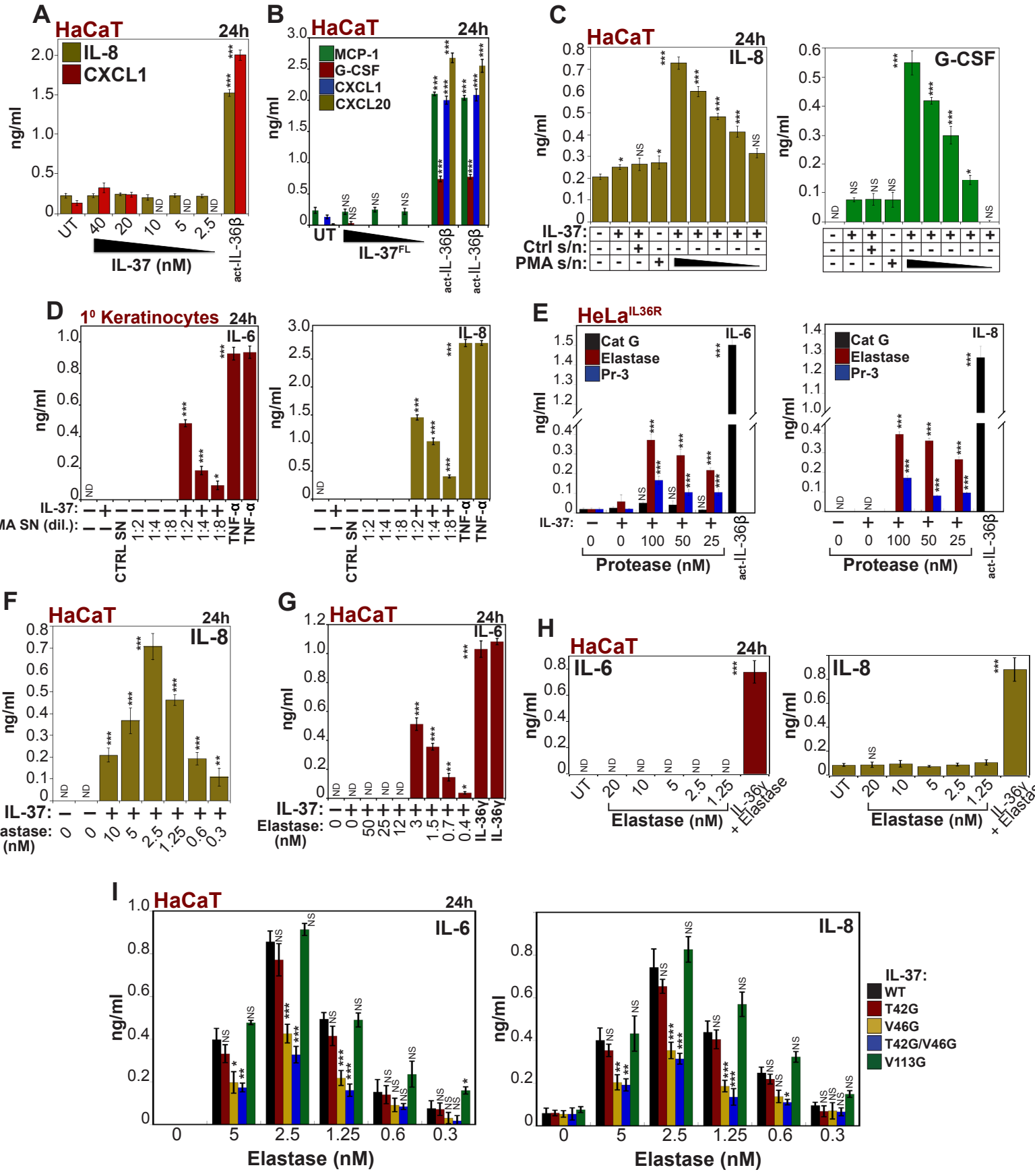
A
HaCaT
24h
IL-8
CXCL1
ng/ml
UT
40
20
10
5
2.5
act-IL-36β
IL-37 (nM)
B
HaCaT
24h
MCP-1
G-CSF
CXCL1
CXCL20
ng/ml
UT
IL-37FL
act-IL-36β
act-IL-36β
C
HaCaT
24h
IL-8
G-CSF
ng/ml
IL-37:
Ctrl s/n:
PMA s/n:
D
1º Keratinocytes
24h
IL-6
IL-8
ng/ml
IL-37:
PMA SN (dil.):
CTRL SN
1:2
1:4
1:8
TNF-α
E
HeLaIL36R
IL-6
IL-8
Cat G
Elastase
Pr-3
ng/ml
IL-37:
0
100
50
25
Protease (nM)
act-IL-36β
F
HaCaT
24h
IL-8
ng/ml
IL-37:
Elastase (nM)
G
HaCaT
24h
IL-6
ng/ml
IL-37:
Elastase (nM)
IL-36γ
IL-36γ
H
HaCaT
24h
IL-6
IL-8
ng/ml
UT
20
10
5
2.5
1.25
Elastase (nM)
IL-36γ + Elastase
I
HaCaT
24h
IL-6
IL-8
ng/ml
Elastase (nM)
IL-37:
WT
T42G
V46G
T42G/V46G
V113G

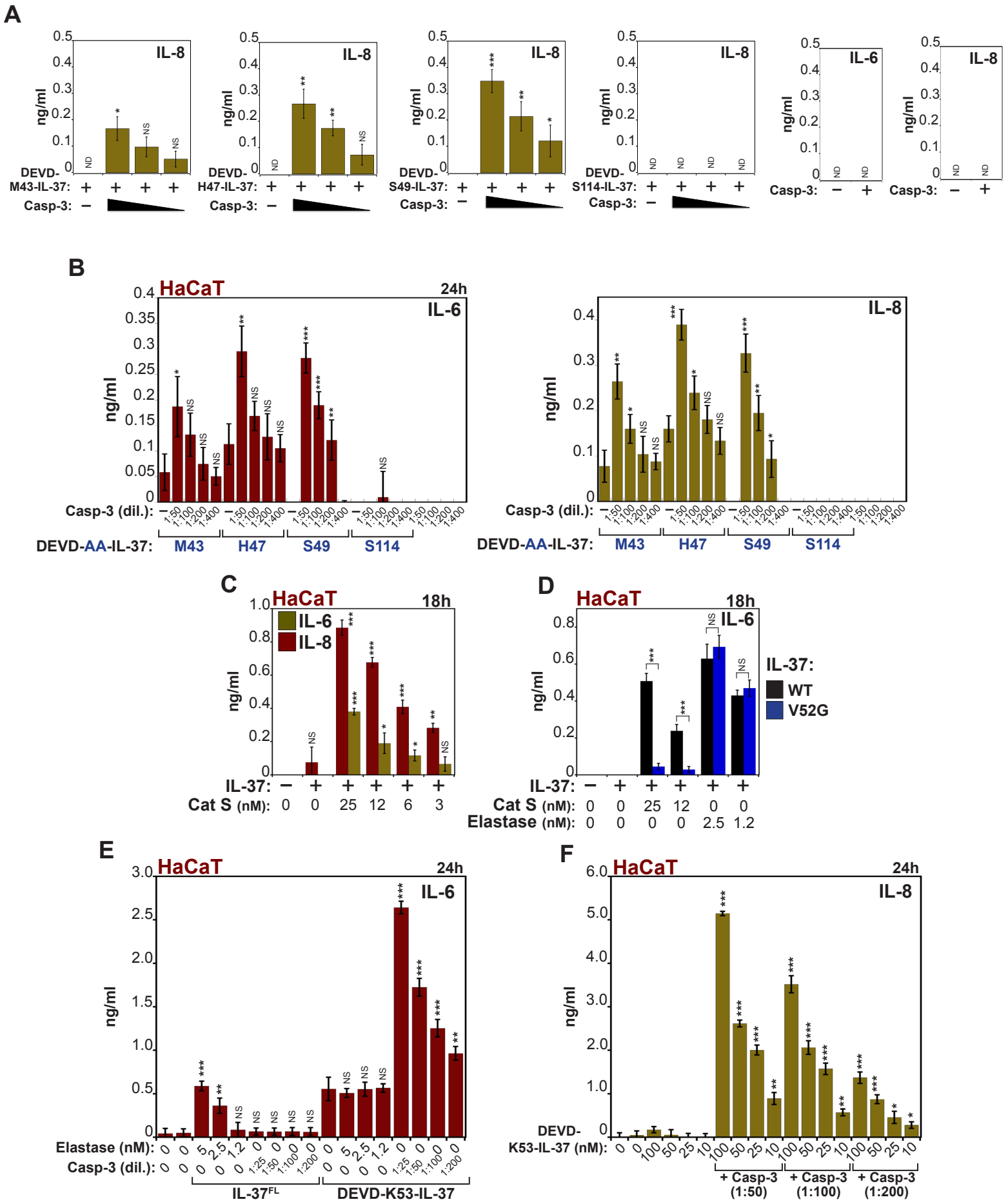
A
IL-8
IL-8
IL-8
IL-8
IL-6
IL-8
ng/ml
DEVD-M43-IL-37:
DEVD-H47-IL-37:
DEVD-S49-IL-37:
DEVD-S114-IL-37:
Casp-3:
ND
NS
B
HaCaT
24h
IL-6
IL-8
ng/ml
Casp-3 (dil.):
DEVD-AA-IL-37:
M43
H47
S49
S114
C
HaCaT
18h
IL-6
IL-8
ng/ml
IL-37:
Cat S (nM):
D
HaCaT
18h
IL-6
IL-37:
WT
V52G
ng/ml
Cat S (nM):
Elastase (nM):
E
HaCaT
24h
IL-6
ng/ml
Elastase (nM):
Casp-3 (dil.):
IL-37FL
DEVD-K53-IL-37
F
HaCaT
24h
IL-8
ng/ml
DEVD-K53-IL-37 (nM):
+ Casp-3 (1:50)
+ Casp-3 (1:100)
+ Casp-3 (1:200)

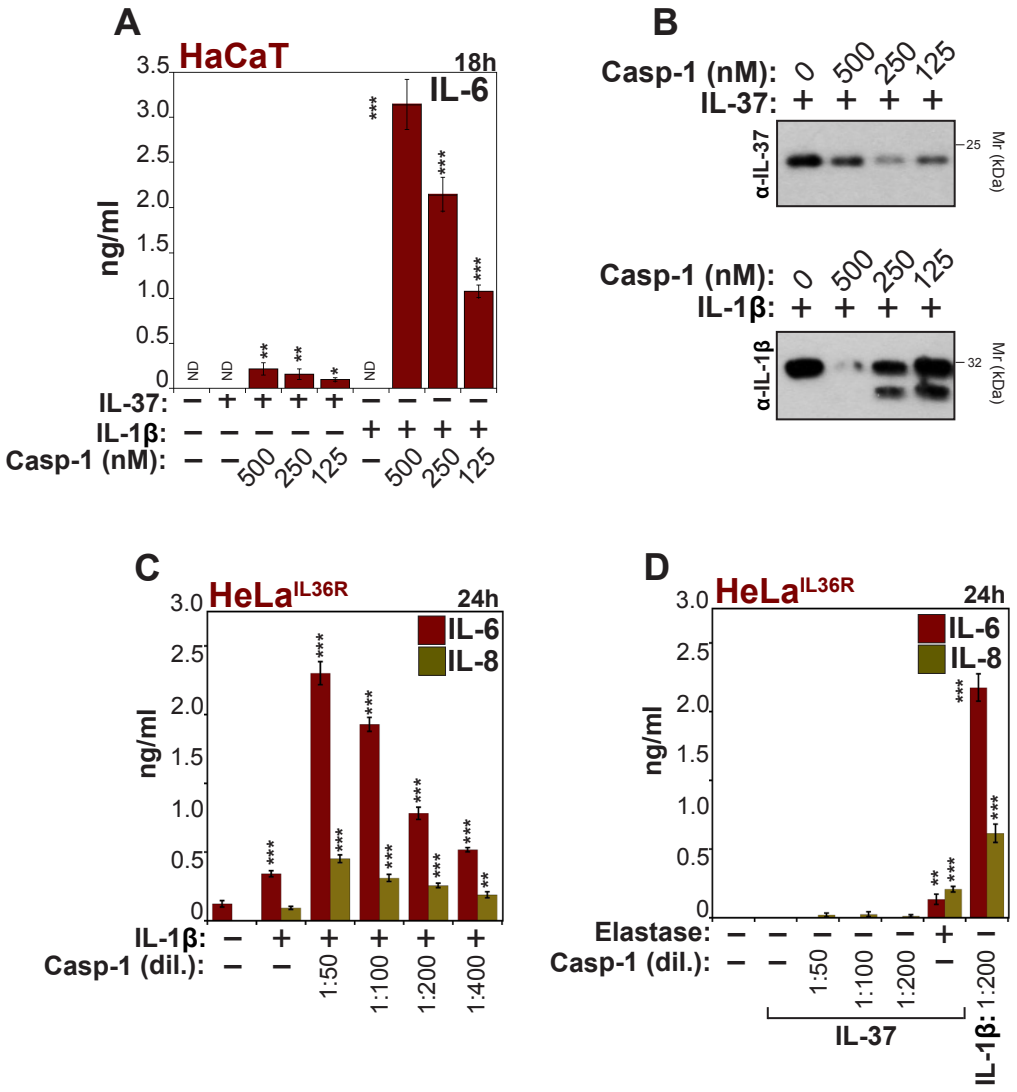
A
HaCaT
18h
IL-6
ng/ml
3.5
3.0
2.5
2.0
1.5
1.0
0.5
0
ND
ND
**
**
*
ND
***
***
***
IL-37: – + + + + – – – –
IL-1β: – – – – – + + + +
Casp-1 (nM): – – 500 250 125 – 500 250 125
B
Casp-1 (nM): 0 500 250 125
IL-37: + + + +
α-IL-37
25
Mr (kDa)
Casp-1 (nM): 0 500 250 125
IL-1β: + + + +
α-IL-1β
32
Mr (kDa)
C
HeLaIL36R
24h
IL-6
IL-8
ng/ml
3.0
2.5
2.0
1.5
1.0
0.5
0
***
***
***
***
***
***
***
***
**
IL-1β: – + + + + +
Casp-1 (dil.): – – 1:50 1:100 1:200 1:400
D
HeLaIL36R
24h
IL-6
IL-8
ng/ml
3.0
2.5
2.0
1.5
1.0
0.5
0
**
***
***
***
Elastase: – – – – – +
Casp-1 (dil.): – – 1:50 1:100 1:200 –
IL-37
IL-1β: 1:200

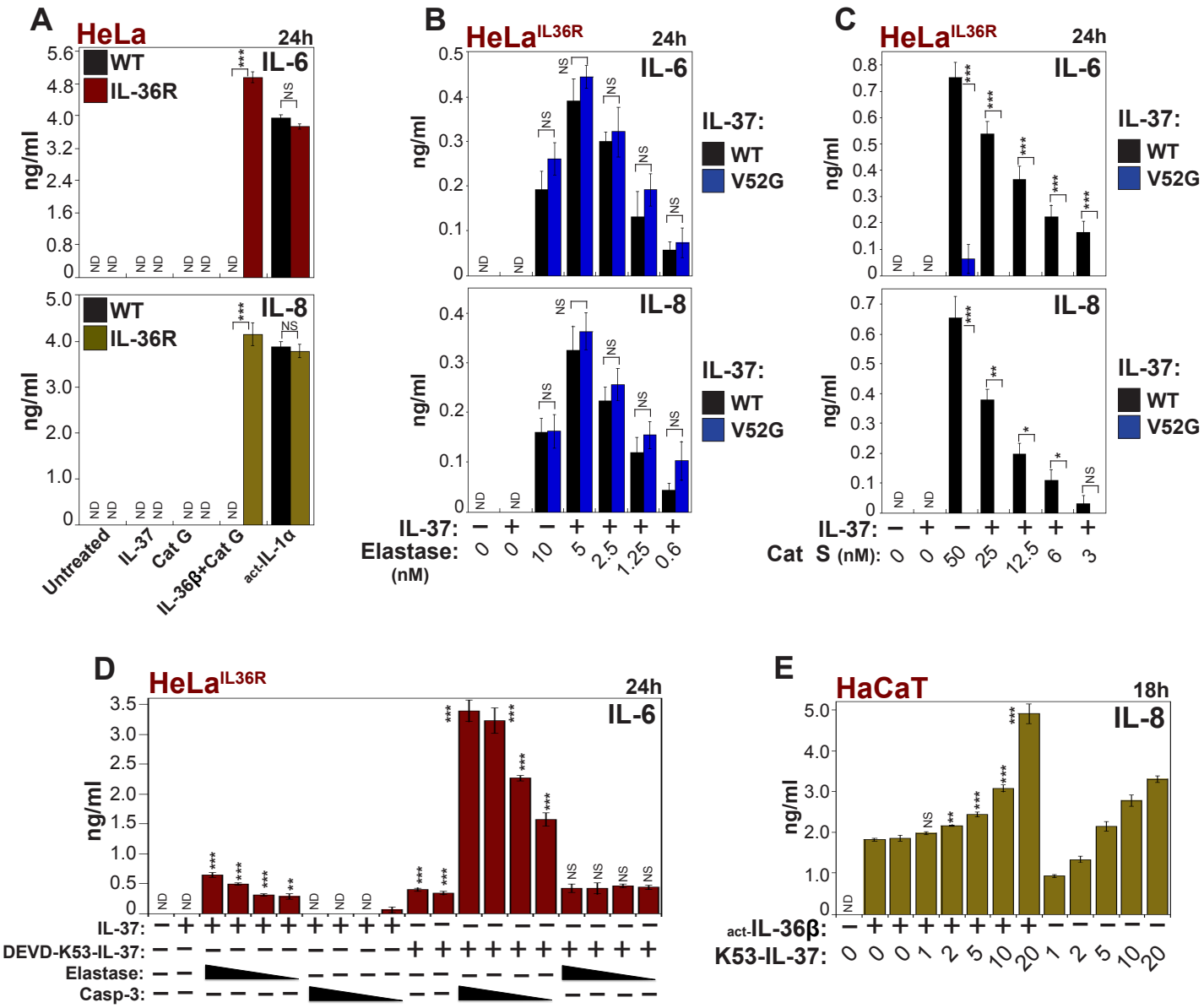
A
HeLa
24h
WT
IL-36R
IL-6
IL-8
ng/ml
Untreated
IL-37
Cat G
IL-36β+Cat G
act-IL-1α
B
HeLaIL36R
24h
IL-37:
WT
V52G
Elastase: (nM)
C
HeLaIL36R
24h
Cat S (nM):
D
HeLaIL36R
24h
IL-37:
DEVD-K53-IL-37:
Elastase:
Casp-3:
E
HaCaT
18h
act-IL-36β:
K53-IL-37:

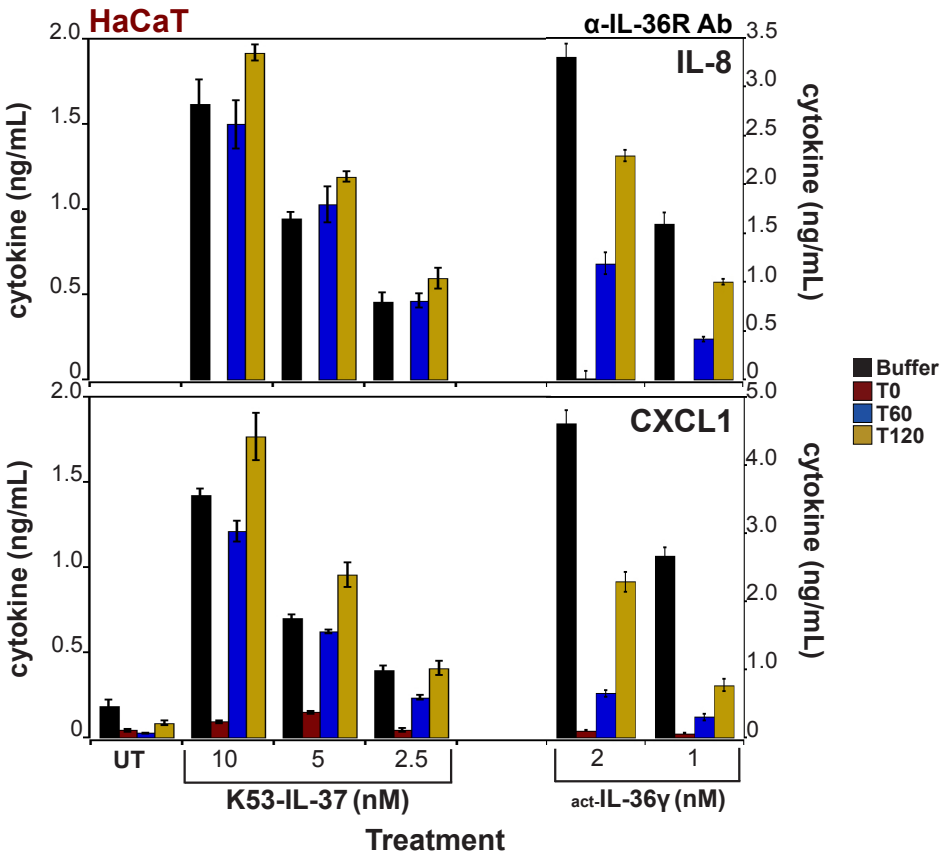
HaCaT
α-IL-36R Ab
IL-8
CXCL1
cytokine (ng/mL)
cytokine (ng/mL)
Buffer
T0
T60
T120
UT
10
5
2.5
2
1
K53-IL-37 (nM)
act-IL-36γ (nM)
Treatment

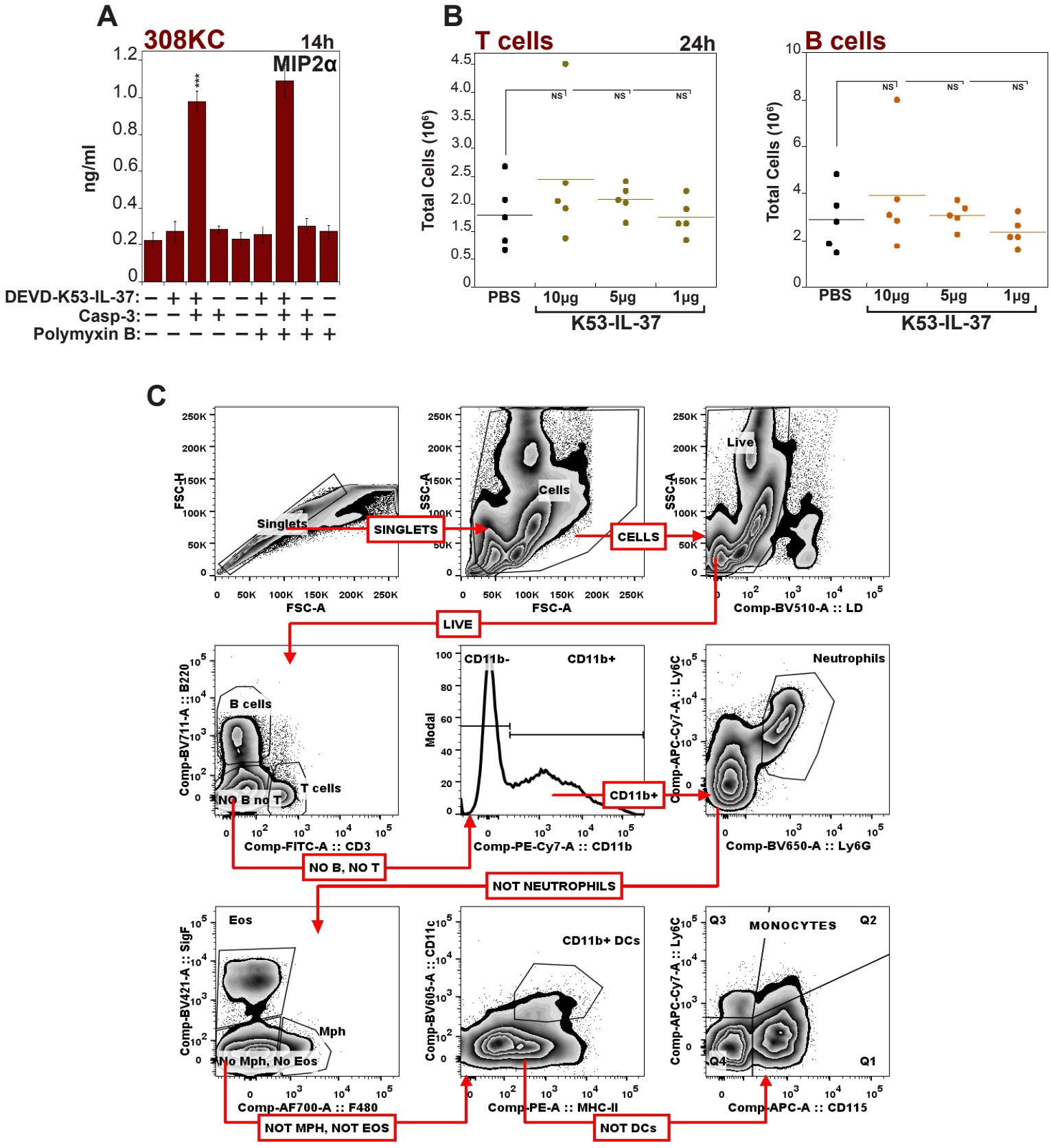
A
308KC
14h
MIP2α
ng/ml
1.2
1.0
0.8
0.6
0.4
0.2
0
***
DEVD-K53-IL-37: – + + – – + + – –
Casp-3: – – + + – – + + –
Polymyxin B: – – – – – + + + +
B
T cells
24h
Total Cells (10⁶)
4.5
4.0
3.5
3.0
2.5
2.0
1.5
1.0
0.5
0
NS
NS
NS
PBS
10µg
5µg
1µg
K53-IL-37
B cells
Total Cells (10⁶)
10
8
6
4
2
0
NS
NS
NS
PBS
10µg
5µg
1µg
K53-IL-37
C
FSC-H
FSC-A
Singlets
SINGLETS
SSC-A
Cells
CELLS
Live
Comp-BV510-A :: LD
LIVE
Comp-BV711-A :: B220
B cells
T cells
NO B no T
Comp-FITC-A :: CD3
NO B, NO T
Modal
CD11b-
CD11b+
Comp-PE-Cy7-A :: CD11b
CD11b+
Comp-APC-Cy7-A :: Ly6C
Neutrophils
Comp-BV650-A :: Ly6G
NOT NEUTROPHILS
Comp-BV421-A :: SigF
Eos
Mph
No Mph, No Eos
Comp-AF700-A :: F480
NOT MPH, NOT EOS
Comp-BV605-A :: CD11c
CD11b+ DCs
Comp-PE-A :: MHC-II
NOT DCs
Q3
MONOCYTES
Q2
Q4
Q1
Comp-APC-A :: CD115